

ATTACHMENT 1

Consumers Power Company
Palisades Plant
Docket 50-255

THE CPCo FULL CORE PIDAL SYSTEM
UNCERTAINTY ANALYSIS

June 25, 1991

50 Pages

9107020010 910625
FOR ADOCK 05000255
P FOR

THE CPCO FULL CORE PIDAL SYSTEM

UNCERTAINTY ANALYSIS

G.A. Baustian
Reactor Engineering
Palisades

REV 0--June 05, 1989 P*PID*89002
REV 1--October 18, 1989 P*PID*89002 Rev 1
REV 2--August 15, 1990 GAB*90*06

ABSTRACT

This report provides an uncertainty analysis for the Palisades Incore Detector Algorithm, PIDAL. A detailed description of the individual uncertainties associated with using the PIDAL methodology for determining the power distribution within the Palisades reactor is presented.

0936 1773

THE GPCO FULL CORE PIDAL SYSTEM

Uncertainty Analysis
REV 2

TABLE OF CONTENTS

- 1- INTRODUCTION
- 2- DESCRIPTION of the STATISTICAL MODEL
- 2.1 Description of Uncertainty Components
 - 2.2 F(s) Uncertainty Component
 - 2.3 F(sa) Uncertainty Component
 - 2.4 F(r) Uncertainty Component
 - 2.5 F(z) Uncertainty Component
 - 2.6 F(l) Uncertainty Component
- 3- CALCULATION of the UNCERTAINTIES
- 3.1 Methodology/Data Base
 - 3.2 Effects of Failed Detectors on Uncertainties
 - 3.3 Effects of Radial Power Tilts on Uncertainties
 - 3.4 Results of Statistical Combinations
- 4- TABLES
- 5- FIGURES
- 6- LIST of REFERENCES
- 7- GLOSSARY

D 9 3 6 1 7 7 4

INTRODUCTION

This report provides an analysis documenting the uncertainties associated with using the Palisades Incore Detector Algorithm, PIDAL, for measuring the full core three dimensional power distribution within the Palisades reactor core (reference #1).

The PIDAL methodology was developed over the course of two years by the Palisades staff with the intention of having the full core PIDAL eventually replace the original Palisades one eighth core INCA model.

Initially, the full core PIDAL solution method was based on a combination of the existing Palisades INCA methodology and other full core measurement schemes. Over the course of development, shortcomings in the previous methods were identified, particularly in the way the full core radial power distributions and tilts were constructed. Several new techniques were employed which resulted in an improved methodology as compared to the previous systems.

In order to determine the uncertainty associated with using the PIDAL system for monitoring the Palisades power distribution, it was again decided to draw on previous industry experience. A copy of the INPAX-II monitoring system uncertainty analysis, developed by Advanced Nuclear Fuels Corporation (formerly Exxon Nuclear) was obtained with the permission of ANF. After preliminary work, the statistical methods used by ANF were deemed adequate, with a few variations, and the uncertainties associated with PIDAL were determined as described by the remainder of this report.

DESCRIPTION of the STATISTICAL MODEL

Section 2.1 Description of Uncertainty Components

As mentioned in the previous section, the desire herein was to determine an uncertainty associated with using the Palisades full core incore analysis model for measuring reactor core power distributions. Therefore, the uncertainties were determined for three different measurement quantities:

$F(q)$, core total peaking factor. Ratio of the peak local pin power to the core average local pin power. For Palisades this value is frequently written in terms of peak linear heat generation rate.

$F(\Delta h)$, integrated pin peaking factor. Ratio of the peak integrated pin power to the core average assembly power.

$F(Ar)$, assembly radial peaking factor. Ratio of the peak assembly power to the core average assembly power.

For each of the parameters defined above, three separate components of the uncertainties associated with the peaking factor calculations are defined. For our purposes these are box measurement, nodal synthesis and pin-to-box uncertainties.

The box measurement component is the uncertainty associated with measuring segment powers in the instrumented detector locations.

The nodal synthesis component is the uncertainty associated with using the radial and axial power distribution synthesis techniques employed by the PIDAL full core model to calculate a nodal power. Specifically, the uncertainties associated with the radial coupling to uninstrumented locations and the axial curve fitting used to obtain an axial power shape from five discrete detector powers.

The pin-to-box uncertainty is the error associated with using the local peaking factors supplied in the vendors physics data library to represent the pin power distribution within each assembly.

With the three uncertainty components defined above, it was necessary to mathematically re-define each of the peaking factors in terms of these components. This was accomplished by utilizing forms for the peaking factors developed by Advanced Nuclear Fuels Corporation (ANF, formerly EXXON Nuclear) for an uncertainty analysis performed on the St. Lucie Unit 1 incore analysis routine, INPAX-II. This analysis is documented by ANF in proprietary report XN-NF-83-01(p) (Reference #2) used by Palisades personnel with the permission of ANF.

DESCRIPTION of the STATISTICAL MODEL

The peaking factors, for purposes of statistical analysis, were written in the following forms:

$$F(q) = F(s)F(r)F(z)F(L) \quad (1)$$

$$F(\Delta h) = F(sa)F(r)F(L) \quad (2)$$

$$F(Ar) = F(sa)F(r) \quad (3)$$

where:

$F(s)$ = Relative power associated with a single incore detector measurement.

$F(sa)$ = Relative power associated with the average of the detector measurements within a single assembly.

$F(r)$ = Ratio of the assembly relative power to the relative power of the detector measurements within the assembly.

$F(z)$ = Ratio of the peak planar power in an assembly to the assembly average power.

$F(L)$ = Peak local pin power within an assembly relative to the assembly average power.

An important point to be drawn from these definitions for the peaking factors is that the $F(r)$ value is equal to the ratio of the assembly relative power to the $F(s)$ or $F(sa)$ value. Thus it should be apparent that the $F(s)$ and $F(sa)$ terms would drop out in a mathematical sense. The $F(s)$ and $F(sa)$ values were retained for the statistical analysis because their respective uncertainties could be calculated directly and used to quantify the box measurement uncertainty. It can be shown that the $F(s)$ or $F(sa)$ terms (denominator) disappear from the $F(r)$ statistical uncertainty term. See section 2.4.

Given the above representations for the three peaking factors of interest, the problem was to develop a method for determining the variance or standard deviation using a combination of the separate uncertainty components. For example, the uncertainty component for $F(Ar)$ is as follows.

The peaking factor, $F(Ar)$, is defined in equation 3 above. Using the general form of the error propagation formula given in Reference #5 P131,

$$S_u^2 = \left(\frac{\partial u}{\partial x}\right)^2 S_x^2 + \left(\frac{\partial u}{\partial y}\right)^2 S_y^2 + \left(\frac{\partial u}{\partial z}\right)^2 S_z^2 + \dots \quad (4)$$

and substituting for u, x and y yields:

$$S_{F(Ar)}^2 = \left(\frac{\partial F(Ar)}{\partial F(sa)}\right)^2 S_{F(sa)}^2 + \left(\frac{\partial F(Ar)}{\partial F(r)}\right)^2 S_{F(r)}^2 \quad (5)$$

DESCRIPTION of the STATISTICAL MODEL

From equation 3 the partial differentials are computed as:

$$\frac{\partial F(Ar)}{\partial F(sa)} = F(r) \quad \text{and} \quad (6)$$

$$\frac{\partial F(Ar)}{\partial F(r)} = F(sa) \quad (7)$$

Substitution of the partials back into (5) gives:

$$S_{F(Ar)}^2 = F(r)^2 S_{F(sa)}^2 + F(sa)^2 S_{F(r)}^2 \quad (8)$$

Dividing both sides of equation 8 by $F(Ar)^2$, which is equivalent to $(F(sa)F(r))^2$, gave an equation for the relative variance for $F(Ar)$ as:

$$\left(\frac{S_{F(Ar)}}{F(Ar)} \right)^2 = \left(\frac{S_{F(sa)}}{F(sa)} \right)^2 + \left(\frac{S_{F(r)}}{F(r)} \right)^2 \quad (9)$$

It is now necessary to find a more convenient form of equation 9 to use for the relative variance of $F(Ar)$. This is done by using the error propagation formula and implementing a simple variable transformation as follows:

$$\text{let } y = \ln(x) \quad \text{and note that } \frac{\partial y}{\partial x} = \frac{1}{x}$$

Substituting into the error propagation formula,

$$S_y^2 = \left(\frac{\partial y}{\partial x} \right)^2 S_x^2 = \left(\frac{1}{x} \right)^2 S_x^2 = \left(\frac{S_x}{x} \right)^2 \quad (10)$$

Note that the form of equation 10 is the same as the form of the individual components of equation 9. Therefore, it is possible to substitute the natural logarithms in the individual variance (or standard deviation) for the actual independent variables. i.e. substitute $\ln(F(s))$ for $F(s)$ in equation 21.

DESCRIPTION of the STATISTICAL MODEL

From the results of equations 9 and 10, the following formulae for the relative sample variances of $F(q)$, $F(\Delta h)$ and $F(Ar)$ can be written:

$$S_{F(q)}^2 = S_{F(s)}^2 + S_{F(r)}^2 + S_{F(z)}^2 + S_{F(L)}^2 \quad (11)$$

$$S_{F(\Delta h)}^2 = S_{F(su)}^2 + S_{F(r)}^2 + S_{F(L)}^2 \quad (12)$$

$$S_{F(Ar)}^2 = S_{F(su)}^2 + S_{F(r)}^2 \quad (13)$$

It should be noted that equations 11, 12 and 13 are valid only by assuming that the individual uncertainty components which make up the overall variance for the peaking factors are independent.

After determining the sample variance for each peaking factor, it is necessary to construct sample tolerance intervals for each estimate. The general form for the tolerance limits is given in Reference #3 page 221, as:

$$\bar{x} \pm KS \quad (14)$$

where

\bar{x} = the estimated sample bias

K = tolerance factor, based on interval size and number of observations

S = estimated sample standard deviation

For our purposes, it is necessary to define only a one-sided tolerance limit. This is because we are trying to quantify how many peaking factor measurements may be below a given limit. In addition, if it can be shown that the overall variance (or standard deviation) for each peaking factor component is made up of normally distributed individual deviations, then the bias term becomes zero. Realizing these two points, equation 14 can be used to construct the following upper tolerance limits for each peaking factor:

$$+K_{F(q)} S_{F(q)} \quad \text{Upper tolerance limit for } F(q) \quad (15)$$

$$+K_{F(\Delta h)} S_{F(\Delta h)} \quad \text{Upper tolerance limit for } F(\Delta h) \quad (16)$$

$$+K_{F(Ar)} S_{F(Ar)} \quad \text{Upper tolerance limit for } F(Ar) \quad (17)$$

For this analysis, a 95/95 tolerance limit is used and appropriate K factors are used to determine the respective one-sided 95/95 tolerance limits. The tolerance factors (K), as a function of degrees of freedom, were taken from Reference #4.

DESCRIPTION of the STATISTICAL MODEL

As mentioned previously, it is necessary to determine the appropriate number of degrees of freedom for each sample standard deviation in order to obtain tolerance factors. This is accomplished by using Satterthwaite's formula which was also used in Reference #2. This formula is given below:

For a variance defined as:

$$S_0^2 = a_1 S_1^2 + a_2 S_2^2 + \dots + a_k S_k^2 \quad (18)$$

The degrees of freedom are given by:

$$df_0 = \frac{S_0^4}{a_1^2 S_1^4 / df_1 + a_2^2 S_2^4 / df_2 + \dots + a_k^2 S_k^4 / df_k} \quad (19)$$

DESCRIPTION of the STATISTICAL MODEL

Section 2.2 F(s) Uncertainty Component

The standard deviation $S_{f(s)}$ is defined as the relative uncertainty in the individual detector segment powers inferred by the full core model. Inferred detector powers are those calculated for uninstrumented assemblies by the full core radial synthesis routine as opposed to detector powers derived directly from the detector signals in instrumented assemblies.

The standard deviation $S_{f(s)}$ can be obtained by comparing equivalent inferred detector powers to powers from already measured, instrumented locations. First, a full core power distribution is obtained based on the full core methodology described in Reference #1. Then, one detector string (consisting of five separate axial operable detectors) is assumed to be failed and the full core radial synthesis routine is repeated. Since the detector locations of the "failed" string are inoperable, the synthesis routine will treat these locations as uninstrumented and independent inferred powers for the once operable string will be obtained.

At this point, the "failed" string is again made operable by using the original detector signals. A second string of five operable detectors is then failed and the solution step repeated. This scheme of failing and replacing operable detector strings is repeated until independent inferred segment powers have been calculated for all operable strings in the reactor. From this scheme, five deviation data points can be obtained for each fully operable string in the core. The whole process is then repeated for roughly fifteen separate power distribution cases from each of Palisades fuel cycles 5, 6 and 7.

The equation for determining the standard deviation of all of the individual segment inferred/measured deviations is as follows:

$$S_{f(s)} = \sqrt{\frac{\sum D^2 - N_s \bar{D}_s^2}{N_s - 1}} \quad (20)$$

where:

N_s = total number of inferred/measured segment power deviations

$$D_{s_i} = \ln(F_{s_i}^I) - \ln(F_{s_i}^M) \quad (21)$$

\bar{D}_s = arithmetic mean of the individual D_{s_i}

$F_{s_i}^M$ = radially normalized measured detector segment power for detector i.

$F_{s_i}^I$ = radially normalized inferred detector segment power for detector i.

DESCRIPTION of the STATISTICAL MODEL

Section 2.2 F(s) Uncertainty Component

It should be noted that there is an underlying assumption made in using equation 20 to determine the individual detector segment power standard deviation. It is assumed that the uncertainty associated with inferring powers in the uninstrumented regions is greater than the uncertainty of the measured detector segment powers from instrumented locations. This assumption is supported by the fact that the inferred detector powers, by design, are influenced by the theoretical solution via the assembly average coupling coefficients. (Section 2.4, Reference #1) Therefore, the inferred detector powers will contain errors induced by the theoretical nodal model.

Initially, this method may appear to not consider any uncertainty components brought about by detector measurement errors and errors in converting the measured detector signals to segment powers. However, the deviations between inferred and measured will in fact contain the measurement uncertainty because the relative difference between measurement and inferred detector segment power represents an estimate of the combined measured and calculational error.

DESCRIPTION of the STATISTICAL MODEL

Section 2.3 F(sa) Uncertainty Component

The standard deviation $S_{f(sa)}$ is defined as the relative uncertainty in the average of the five inferred detector segment powers within an assembly. The inferred and measured detector segment power data used for this component comes from the same individual segment power data used for the $S_{f(s)}$ analysis.

The equation used for determining the standard deviation of the string-average detector segment inferred/measured deviations is:

$$S_{f(sa)} = \sqrt{\frac{\sum D_{sai}^2 - N_{sa} \bar{D}_{sa}^2}{N_{sa} - 1}} \quad (22)$$

where:

N_{sa} = total number of inferred/measured average segment power deviations.

$$D_{sai} = \ln(F_{sai}^I) - \ln(F_{sai}^M) \quad (23)$$

\bar{D}_{sa} = arithmetic mean of the individual D_{sai}

F_{sai}^M = average of the radially normalized measured detector segment powers for detector string i.

F_{sai}^I = average of the radially normalized inferred detector segment powers for detector string i.

DESCRIPTION of the STATISTICAL MODEL

Section 2.4 F(r) Uncertainty Component

The standard deviation $S_{F(r)}$ is defined as the relative uncertainty associated with the radial synthesis from instrumented assembly powers to assembly powers for uninstrumented assemblies. This component assumes that the radial coupling methods employed are valid and accurate for inferring detector powers in uninstrumented assemblies, and that the resultant integrated assembly powers are similar to known values.

The data for this component is obtained by starting with a theoretical XTG quarter core power distribution and obtaining from this equivalent detector powers. Note that these theoretical detector powers are already calculated in the full core model for other uses. These detector powers can then be used as the detector data input to the corresponding full core case. The PIDAL model will then calculate a full core power distribution based on the XTG detector powers. The resultant integrated assembly powers are then compared with the original radial power distribution supplied by XTG. The difference will represent the error in the radial synthesis method.

The equation used for calculating the $S_{F(r)}$ standard deviation is:

$$S_{F(r)} = \sqrt{\frac{\sum D_{r_i}^2 - N_c \bar{D}_c^2}{N_c - 1}} \quad (24)$$

where:

N_c = total number of PIDAL/XTG assembly powers compared

$$D_{r_i} = \ln(F_{r_i}^F) - \ln(F_{r_i}^M) \quad (25)$$

\bar{D}_c = arithmetic mean of the individual D_{r_i}

$F_{r_i}^F$ = core normalized PIDAL F(r) peaking factor calculated by the full core model for assembly i

$F_{r_i}^M$ = core normalized (original) XTG F(r) peaking factor for assembly i

As mentioned in section 2.1, the F(r) uncertainty term is mathematically the ratio of assembly relative power to the power of the detector measurements in an assembly. From equation 25, it can be shown that the detector measurement term (either F(s) or F(sa)) drops out of the formulation. This is because the difference in the natural logarithms is identically equal to the natural logarithm of the inferred F(r) term divided by the measured F(r) term. Thus the denominators of each term would cancel out.

DESCRIPTION of the STATISTICAL MODEL

Section 2.5 F(z) Uncertainty Component

The standard deviation $S_{F(z)}$ is defined as the relative uncertainty associated with the axial synthesis from five detector segment powers to twenty-five axial nodal powers. This is the uncertainty associated with the axial curve fitting technique, including calculation of axial boundary conditions, employed by the Palisades full core model.

The data for this component is obtained by starting with a theoretical XTG quarter core power distribution and detector powers as discussed for the F(r) component. The XTG detector powers were again used as the detector data input to a corresponding full core case. The PIDAL model then calculates a full core power distribution based on the XTG detector powers. The resultant assembly normalized axial peaking factors obtained by PIDAL are then compared with the original XTG axial peaking factors for each quarter core location.

The equation used for calculating the $S_{F(z)}$ standard deviation is:

$$S_z = \sqrt{\frac{\sum D_{zi}^2 - N_z \bar{D}_z}{N_z - 1}} \quad (26)$$

where:

N_z = total number of inferred/XTG F(z) axial peaks compared

$$D_{zi} = \ln(F_{zi}^I) - \ln(F_{zi}^M) \quad (27)$$

\bar{D}_z = arithmetic mean of the individual D_{zi}

F_{zi}^I = assembly normalized F(z) peaking factor calculated by the full core model for assembly i

F_{zi}^M = assembly normalized (original) XTG F(z) peaking factor for assembly i

DESCRIPTION of the STATISTICAL MODEL

Section 2.6 F(1) Uncertainty Component

The standard deviation $S_{F(L)}$ is defined as the uncertainty associated with pin-to-box factors supplied to PIDAL in the fuel vendors cycle dependent data library. This factor is the ratio of assembly peak pin power to average power for that assembly. These factors are supplied by the fuel vendor (Advanced Nuclear Fuels Corporation) and come from quarter core PDQ models used by ANF in the Palisades reload design process.

The value of $S_{F(L)}$ can be obtained from ANF. The value currently used by ANF, as determined for Westinghouse PWR's, and Combustion Engineering PWR's with 14X14 assemblies is .0135.

Because Palisades has cruciform control rods and thus there are wide-wide, narrow-wide, and narrow-narrow water gaps surrounding the Palisades assemblies, there is some concern that the same value for $S_{F(L)}$ can be used. It was determined however, that the previously derived ANF pin-to-box uncertainty component could be used herein for the following two reasons.

The ANF cycle dependent pin-to-box factor are generated using PDQ methods that are consistent with other reactors for which ANF supplies physics data. Therefore, it is expected that the error in pin powers calculated by ANF for Palisades will be similar to the error that ANF has derived for other PWR's.

Secondly, concern over the ability of a two-group PDQ model to accurately describe the local power distributions in the regions of the differing water gaps prompted an agreement between the NRC, CPCo and ANF to have ANF use a four group PDQ model for Palisades design work. It is reasonable to assume that a four group PDQ model for Palisades will be at least as accurate as a two-group model for other PWR's. Therefore, the ANF value of $S_{F(L)} = .0135$ will be used for this analysis.

CALCULATION of the UNCERTAINTIES

Section 3.1 Methodology/Data Base

Four steps were taken in order to determine the uncertainties associated with the PIDAL full core monitoring model. The first step consisted of defining an appropriate statistical model. This was done as described by Section 2.

The second and third steps consisted of generating the computer software necessary for implementing the statistical model and running the necessary computer cases. These steps are described in this section.

Finally, it was necessary to take the results of the computer cases and combine them in order to determine the overall uncertainties as defined by the statistical model. Included in this step was a study of the effects of failing large numbers of incore detectors, as well as an investigation into the effect of radial power tilts on the PIDAL methodology. The results of this step are discussed in Sections 3.2 through 3.4.

Three computer codes were used for the statistical analysis work performed. The following brief descriptions apply.

The PIDAL main program was used to determine the measured and inferred full core detector powers and power distributions required. The PIDAL program was described in detail by Reference #1.

The BDSTAT program was used to calculate the $F(s)$, $F(sa)$ and $F(r)$ uncertainty components. This program reads output files generated by the PIDAL program statistical analysis routines and calculates the deviations, means and standard deviations required by this analysis. BDSTAT also sets up histogram data files for figure plotting.

The STATFZ program was used to calculate the $F(z)$ uncertainty component. This program reads output from the PIDAL exposure data file and calculates $F(z)$ deviations and statistics between the stored PIDAL and XTG values. STATFZ also sets up a histogram data file for plotting.

The data base used for this analysis was generated using measured and predicted power distributions for Palisades cycles 5, 6 and 7. For the $F(s)$, $F(sa)$ and $F(r)$ uncertainty components a total of 54 PIDAL cases, equally distributed over the three cycles, were run. The cases used were selected from Reference #7. Since Reference #7 contained twice as many cases as were statistically necessary, it was decided to use only half of the cases so only every other case was selected. Tables #1, #2 and #3 list the cases which were run using the PIDAL statistical analysis option for cycles 5, 6 and 7, respectively.

CALCULATION of the UNCERTAINTIES

Section 3.1 Methodology/Data Base

Three separate cycle 7 BDSTAT statistical runs were performed. The first considered the entire compliment of detector data, including fresh and reused incores, and the original cycle 7 INCA W' signal-to-box power conversion library. This library was revised by ANF which resulted in a second set of statistical data. A third cycle 7 set was then generated which omitted the reused detectors from the cycle 7 data. Note that the statistics from the first cycle 7 BDSTAT run are for information only.

A total of 22 PIDAL cases were run in order to generate data for the PIDAL F(z) uncertainty component. Of these 22 cases, 11 were selected from the cycle 7 INCA run log. These 11 cases were selected at approximately equal intervals over the fuel cycle. Also part of the total 22 cases were 11 cases run from a hypothetical EOC 7 Xenon oscillation. These cases were selected in order to include off-normal axial power shapes in the uncertainty analysis. Table #4 lists the cases used for the F(z) uncertainty component.

One concern was the fact that the "known" axial power shapes which were to be reconstructed using PIDAL came from XTG solutions. This was a problem because XTG does not account for slight flux depressions caused by fuel assembly spacer grids. It is reasonable to assume that axial peaking uncertainties caused by these types of flux disturbances would be small, compared to the off-normal axial shapes being investigated, and therefore these fluxuations were ignored by this analysis.

A total of 18 PIDAL cases were run in order to determine the measurement uncertainties for radially tilted cores. All of these PIDAL cases used theoretical detector powers from two full core XTG dropped rod induced transient scenarios. One of these (used for the first six PIDAL cases) was induced by dropping a group 4 control rod, while the other (used for the second six PIDAL cases) used a group 3-outer rod as initiator.

The first six PIDAL cases run corresponded to peak quadrant power tilts of 10%, 7.6%, 5.6%, 2.9%, 1.6% and 0.3% respectively. These cases were selected because they covered the spectrum of tilted cores for a tilt range of no tilt up to 10% tilt. Concentration on tilts between 0% and ~5% was greater because it is over this range that the operator may be operated without reducing power or correcting the tilt. The second six PIDAL cases all lie within the no tilt and ~5% quadrant power tilt range.

There were two reasons for using the two different transient scenarios as suppliers of the theoretical detector powers. First, the dropped group 3-outer rod scenario did not result in quadrant power tilts greater than 5% during the oscillatory period. Therefore, it was necessary to use cases from the dropped group 4 rod scenario in order to get results on tilts up to 10%. Secondly, the oscillations between the two scenarios were quite different. The dropped group 3-outer rod oscillated about the major symmetric axis while the dropped group 4 rod scenario oscillated about the diagonal axis. Consideration of both is important because the majority of the symmetric incore detector locations are rotationally symmetric (and not generally symmetric about either major axis or diagonal) and therefore oscillations about differing axis' could have differing effects on the accuracy of the PIDAL quadrant power tilt algorithm.

177
0986

CALCULATION of the UNCERTAINTIES

Section 3.1 Methodology/Data Base

Expanding on this last statement, it was decided to further investigate the effects of tilt location on the PIDAL solution. In the case of the dropped group 4 rod induced transient, the power peak used for the PIDAL cases 1 through 6 occurred in quadrant 2. What if the power peak was in one of the other three quadrants? In other words, what if the power distribution was the same, just rotated 90, 180 or 270 degrees? Since the incore detectors are not equally distributed over the quadrants, it is not expected that the power distributions as measured by PIDAL would be the same for the rotated cases. The same questions can be asked for the group 3-outer rod induced transient as well.

Six additional PIDAL cases were then run. Three of the cases were for the 5% tilted group 4 rod induced oscillation at rotations of 90, 180 and 270 degrees clockwise from the original power distribution. The other three cases were for the 5% tilted group 3-outer rod induced transient at rotations of 90, 180 and 270 degrees.

0936 1777

CALCULATION of the UNCERTAINTIES

Section 3.2 Effects of Failed Detectors on Uncertainties

Current Palisades Technical Specifications require that 50% of all possible incore detector locations, with a minimum of two incore detectors per core level per quadrant be working in order to declare the incore monitoring system operable. A look at current Combustion Engineering standard technical specifications revealed that the current standard is for 75% of the possible incore locations be operable. It is assumed that the CE standard is referring to plants which incorporate the standard CE full core monitoring methodologies.

It is anticipated that the Palisades technical specifications will be revised to reflect the current CE standard once the PIDAL methodology becomes production. In order to make this change, the study described by this section was necessary in order to justify the 75% operability value which will be used.

In Reference #2, ANF came to the conclusion that the accuracy of an incore monitoring system or methodology depended more on which instruments were operable than on the total number operable. ANF also concluded that it was best to use all available data points in determining the individual uncertainties and therefore did not go into great detail investigating the effects of large numbers of incore failures on the measured/inferred power distribution. These conclusions are valid because, for random detector failures, there is an equal probability that the well behaved detectors and the non-well behaved detectors would fail.

In order to prove these conclusions it would be necessary to test every possible combination of failed detectors for a large set of power distributions. From a computational standpoint, this would not be practical. Therefore, two tests were devised in order to verify that incore failures resulting in only 75% detector operability would produce accurate measurements.

The first test consisted of verifying the $F(sa)$ and $F(s)$ uncertainty components for measurements with 11 incore strings (55 total detectors) failed. This failure rate, 25.6% of 215, was chosen because of its consistency with current standard technical specifications. Cycle 6 PIDAL case #5 was chosen as the base case to this test. The $S_{f(sa)}$ and $S_{f(s)}$ component uncertainties for this case were found to be 0.0134 and 0.0299, respectively. See Table #6. Five sets of eleven failed incore strings were then chosen using a random number generator and input to PIDAL. The statistical analysis was repeated for each of the five failed sets. The resultant $S_{f(sa)}$ and $S_{f(s)}$ components were found to be 0.0171 and 0.0328, respectively. Statistical peaking factor uncertainties were then determined based on the base case and 25% failure rate case. From these calculations, penalty factors accounting for the apparent measurement degradation based on detector failures were derived. These penalty factors were then applied to the uncertainties derived from the full data base.

CALCULATION of the UNCERTAINTIES

Section 3.2 Effects of Failed Detectors on Uncertainties

The first test was then repeated for an off-normal power distribution case. The PIDAL base case was a dropped rod measurement from cycle 7. The base case uncertainty components for this case were $S_{f(sa)} = 0.0812$ and $S_{f(s)} = 0.0955$. Five new random sets of 11 incore strings to be failed were generated and the statistics calculations repeated. The resultant $S_{f(sa)}$ and $S_{f(s)}$ were 0.1293 and 0.1369, respectively. From these results, it is clear that PIDAL does not handle large local perturbations such as a dropped rod with a high degree of certainty.

There are two reasons why the dropped rod case resulted in higher measurement uncertainties. The W' data used by PIDAL, and most other monitoring systems as well, comes from steady state PDQ (or similar) calculations. Therefore, the detector signal-to-power conversion is not very accurate for this type of case. Secondly, and more importantly, the coupling coefficients used by PIDAL are inferred based on one-quarter core measured and theoretical detector powers. These coupling coefficients have no way of compensating for gross full core asymmetries such as a dropped control rod.

Palisades plant procedures currently state that the incore monitoring system can not be used for verifying core peaking factors in the event of a dropped or misaligned control rod. At this time, there is no intention of revising these procedures to the contrary until a full core coupling coefficient methodology, capable of accounting for large local reactivity perturbations has been added to PIDAL. Work is underway to develop such a methodology.

A second test was devised in order to further study the effects of gross incore failures on the PIDAL methodology. This test consisted of failing large quantities of incores on an individual basis (not by string) and quantifying the resultant effects on the PIDAL measurements.

The base case for this test consisted of a typical run from cycle 8 in which 206 of 215 possible incores were operable. Five sets of 54 (25%) failed incores were generated using a random number generator. The PIDAL power distribution was then re-calculated for each of the five sets of failures, with the resultant integrated assembly powers compared back to the base case. This test was then repeated for failure thresholds of 50% and 75% failed incores.

Average assembly power deviations were found to be 0.60%, 1.10% and 1.57% for the 25%, 50% and 75% failed incore detector cases respectively. From these results it is clear that as additional incore detectors are failed, the power distribution as measured by PIDAL tends to depart from the base case. From the individual cases, it is also apparent that the degree of agreement between the test cases and base case depends strongly on which incore detectors are operable. An example of this is the spread between the average deviations for the five 25% cases which had a high case average of 0.71% and a low of 0.45%.

Based on these results, it is safe to assume that the uncertainties associated with the PIDAL system documented by this report are valid for an incore monitoring system operable with up to 25% of it's 215 incore detector considered failed. It is also apparent that detector failure rates greater than 25% have an adverse effect on PIDAL's ability to determine the measured power distribution.

CALCULATION of the UNCERTAINTIES

Section 3.3 Effects of Radial Power Tilts on Uncertainties

This section is a summary of work performed as documented in Reference #8, which should be consulted if further detail is required.

The purpose of the work described by Reference #8 was to determine the F(s) uncertainty component for radially perturbed or tilted power distributions up to the full power Technical Specification Limit of 5% quadrant power tilt.

The F(s) uncertainty component was recalculated for radially tilted cores. It was found that in all cases the F(s) uncertainty component for tilted cores was bounded by the value assumed for the whole data base (0.0277) for quadrant power tilts up to 2.8%. It was also found that the value of the F(s) uncertainty component depended strongly on the direction and magnitude of the oscillation causing the power tilt. For cores oscillating about the diagonal core axis, the 0.0277 value is valid for tilts up to 5%.

For oscillations about the major core axis, the F(s) uncertainty component ceases to be bounded by the 0.0277 value for quadrant power tilts greater than 2.8%. Since the Palisades Technical Specifications allow for full power operation with quadrant power tilts of up to 5%, and it was clear that the overall PIDAL uncertainties were only valid for tilts up to 2.8%, it was necessary to derive new uncertainties to allow use of PIDAL for tilts above 2.8%. The new uncertainties were derived and the results may be found in Table #12.

0986 1773

CALCULATION of the UNCERTAINTIES

Section 3.4 Results of Statistical Combinations

Tables #5 through #9 contain the results of the $F(s)$, $F(sa)$ and $F(r)$ statistical calculations for fuel cycles 5,6 and 7. Table #8 shows the original cycle 7 results assuming reused incore detectors. Table #9 shows analogous cycle 7 data with the reused incore data omitted. Table #10 shows a summary totaling all of the $F(s)$, $F(sa)$ and $F(r)$ data for all three fuel cycles assuming no reused incore detectors.

Figures #1 through #15 are deviation histograms corresponding to the data used for the $F(s)$, $F(sa)$ and $F(r)$ standard deviations. From the histograms and means presented, it is apparent that the data is normal and unbiased. One interesting point to note is that the $F(r)$ data is not biased as ANF had found it to be. They explained their bias as being induced by using data sets that were not normalized. The PIDAL data used was radially normalized so the PIDAL result seems to support the ANF assumption.

Table #11 contains the results of the $F(z)$ statistical calculations using cycle 7 data. The first 11 elements of Table #11 were taken from the simulated Xenon oscillation data. The last 11 elements correspond to "typical" data equally spread out through cycle 7. Note that element 20 was from a dropped rod transient. Figure #16 shows a histogram for the $F(z)$ deviation data. From this histogram, the data appears generally normal but the mean deviation indicates a bias of 0.9%. Since this bias is positive, the PIDAL model is over-predicting the peak and is therefore conservative. This is similar to the result obtained by ANF.

Three sets of tolerance limits were determined for $F(q)$, $F(h)$ and $F(Ar)$. The first set is based on theoretical data and is valid when quadrant power tilt, as measured by PIDAL, exceeds 2.8%. The second set is based entirely on cycle 7 data and is valid only for reload cores which contain fresh and once-burned incore detectors. The third set of tolerance limits is based on data from all three cycles, excluding the cycle 7 reused detector data, and is valid only for reload cores with all fresh incore detectors.

Table #12 contains a summary of all of the statistical uncertainty values obtained. From this table, the one-sided 95/95 tolerance limits associated with Palisades PIDAL model were found to be: 0.0623 for $F(q)$, 0.0455 for $F(h)$ and 0.0401 for $F(Ar)$ for un-tilted cores with all fresh incore detectors. For cores using a mixture of fresh and once-burned incore detectors, the 95/95 tolerance limits for $F(q)$, $F(h)$ and $F(Ar)$ were found to be 0.0664, 0.0526 and 0.0490 respectively. Finally, for measurements when quadrant power tilt as measured by PIDAL exceeds 2.8%, the 95/95 tolerance limits for $F(q)$, $F(h)$ and $F(Ar)$ were found to be 0.0795, 0.0722 and 0.0695, respectively.

0936 1779

TABLES

PIDAL Run Number	Exposure MWD/MT	Rx. Power MWth
1	0.0	1694
2	224.5	2419
3	520.2	2300
4	944.9	2321
5	1504.6	2494
6	2287.7	2515
7	3007.9	2514
8	4235.7	2509
9	5338.2	2496
10	6424.1	2499
11	7248.3	2524
12	8099.9	2518
13	9187.2	2504
14	10068.5	2525
15	10850.1	2497
16	11721.9	2480
17	12127.1	2227
18	12487.6	1849

Table #1—Cycle 5 PIDAL case exposures and powers for F(s),
F(sa) and F(r) uncertainty components.

TABLES

PIDAL Run Number	Exposure MWD/MT	Rx. Power MWth
19	0.0	1160
20	135.9	1992
21	370.6	2542
22	1051.6	2464
23	1840.3	2456
24	2845.5	2456
25	3527.1	2460
26	4180.8	2477
27	4533.1	2460
28	5618.9	2468
29	6489.7	2457
30	6881.2	2468
31	7963.9	2455
32	8282.6	2240
33	9080.0	2467
34	9832.7	2483
35	10300.2	2464

Table #2—Cycle 6 PIDAL case exposures and powers for F(s),
F(sa) and F(r) uncertainty components.

TABLES

PIDAL Run Number	Exposure MWD/MT	Rx. Power MWth
36	859.8	2475
37	1293.7	2453
38	0.0	782
39	143.0	2406
40	265.8	2462
41	519.3	1341
42	1596.7	1892
43	2310.7	2514
44	2974.1	2535
45	3994.4	2529
46	5219.7	2357
47	6615.5	2527
48	7386.0	2531
49	8226.8	2537
50	8922.9	2526
51	9837.4	2529
52	10468.8	2528
53	11105.8	2409
54	11556.4	2406

Table #3—Cycle 7 PIDAL case exposures and powers for $F(s)$,
 $F(sa)$ and $F(r)$ uncertainty components.

TABLES

PIDAL Run Number	Exposure MWD/MT	Rx. Power MWth	% Axial Offset
1	172.9	2397	- 1.8
2	1075.7	2476	- 0.7
3	1437.3	2512	0.1
4	1807.2	2476	- 0.1
5	2974.1	2530	1.4
6	3994.4	2529	2.5
7	5930.1	2518	3.8
8	7386.0	2525	4.0
9	8683.3	1142	-18.3
10	9364.5	2526	3.5
11	10468.8	2528	3.2
12	10510.7	2528	-40.0
13	10513.3	2528	-32.7
14	10514.6	2528	-27.6
15	10515.9	2528	-21.4
16	10517.3	2528	-13.9
17	10518.6	2528	- 5.1
18	10519.9	2528	4.5
19	10521.2	2528	14.4
20	10522.5	2528	23.4
21	10523.9	2528	30.5
22	10527.8	2528	39.2

Table #4--Cycle 7 PIDAL runs used for F(z) uncertainty components.

SUMMARY EDIT FOR ALL CASES THIS RUN
 CASE AVERAGE SEGMENT RMS SEGMENT
 DEVIATION % DEVIATION

			F(S) ST. DEV.	F(S) OBSERV.	F(SA) ST. DEV.	F(SA) OBSERV.	F(R) ST. DEV.	F(R) OBSERV.
1	0.44	3.30	0.0324	195.	0.0216	39	0.0021	51.
2	0.38	2.61	0.0259	190.	0.0200	38	0.0021	51.
3	0.33	2.56	0.0254	195.	0.0199	39	0.0018	51.
4	0.32	2.66	0.0264	190.	0.0208	38	0.0018	51.
5	0.22	3.60	0.0356	169.	0.0256	33	0.0023	51.
6	0.24	2.81	0.0282	165.	0.0210	33	0.0024	51.
7	0.19	3.09	0.0314	164.	0.0253	32	0.0024	51.
8	0.19	2.67	0.0266	177.	0.0227	35	0.0024	51.
9	0.21	2.94	0.0295	177.	0.0258	35	0.0023	51.
10	0.11	2.66	0.0268	177.	0.0229	35	0.0025	51.
11	0.11	2.74	0.0271	177.	0.0227	35	0.0026	51.
12	0.14	2.93	0.0293	167.	0.0251	33	0.0026	51.
13	0.24	2.76	0.0275	158.	0.0228	31	0.0026	51.
14	0.17	3.23	0.0311	152.	0.0251	30	0.0024	51.
15	-0.05	3.26	0.0324	148.	0.0270	29	0.0023	51.
16	-0.01	2.80	0.0280	160.	0.0239	32	0.0022	51.
17	-0.05	3.41	0.0341	172.	0.0280	34	0.0021	51.
18	-0.01	2.94	0.0291	161.	0.0255	32	0.0021	51.

F(S) STANDARD DEVIATION ALL CASES = 0.0293 MEAN = 0.0014 DEGREES OF FREEDOM = 3094.

F(SA) STANDARD DEVIATION ALL CASES = 0.0233 MEAN = 0.0014 DEGREES OF FREEDOM = 619.

F(R) STANDARD DEVIATION ALL CASES = 0.0023 MEAN = 0.0000 DEGREES OF FREEDOM = 918.

TABLE 5 - CYCLE 5 F(s), F(sa) and F(r) Data

SUMMARY EDIT FOR ALL CASES THIS RUN
CASE AVERAGE SEGMENT RMS SEGMENT
DEVIATION %DEVIATION

			F(S) ST. DEV.	F(S) OBSERV.	F(SA) ST. DEV.	F(SA) OBSERV.	F(R) ST. DEV.	F(R) OBSERV.
1	0.04	3.29	0.0336	152.	0.0182	30	0.0017	51.
2	0.01	3.09	0.0314	163.	0.0149	32	0.0018	51.
3	0.00	2.90	0.0294	168.	0.0130	33	0.0015	51.
4	-0.03	3.06	0.0314	175.	0.0136	35	0.0016	51.
5	-0.01	2.94	0.0299	175.	0.0134	35	0.0020	51.
6	-0.08	2.67	0.0267	170.	0.0114	34	0.0022	51.
7	-0.15	2.38	0.0238	155.	0.0114	31	0.0022	51.
8	-0.15	2.37	0.0236	160.	0.0110	32	0.0023	51.
9	-0.10	2.42	0.0242	160.	0.0114	32	0.0023	51.
10	-0.14	2.29	0.0228	160.	0.0108	32	0.0024	51.
11	-0.17	2.28	0.0226	155.	0.0107	31	0.0023	51.
12	-0.15	2.22	0.0221	155.	0.0106	31	0.0026	51.
13	-0.23	2.79	0.0283	145.	0.0123	29	0.0026	51.
14	-0.06	3.13	0.0318	140.	0.0130	28	0.0028	51.
15	-0.15	2.97	0.0306	152.	0.0132	30	0.0028	51.
16	-0.18	2.34	0.0241	152.	0.0124	30	0.0025	51.
17	-0.23	2.37	0.0244	152.	0.0126	30	0.0026	51.

F(S) STANDARD DEVIATION ALL CASES = 0.0272 MEAN = -.0013 DEGREES OF FREEDOM = 2689.

F(SA) STANDARD DEVIATION ALL CASES = 0.0125 MEAN = -.0014 DEGREES OF FREEDOM = 538.

F(R) STANDARD DEVIATION ALL CASES = 0.0023 MEAN = -.0001 DEGREES OF FREEDOM = 867.

TABLE 6- CYCLE 6 F(s), F(sa) and F(r) Data

SUMMARY EDIT FOR ALL CASES THIS RUN
 CASE AVERAGE SEGMENT RMS SEGMENT
 DEVIATION %DEVIATION

			F(S) ST. DEV.	F(S) OBSERV.	F(SA) ST. DEV.	F(SA) OBSERV.	F(R) ST. DEV.	F(R) OBSERV.
1	0.30	3.14	0.0310	180.	0.0245	36	0.0014	51.
2	0.49	3.60	0.0350	185.	0.0269	37	0.0015	51.
3	0.41	3.88	0.0382	175.	0.0225	35	0.0018	51.
4	0.36	3.61	0.0354	180.	0.0244	36	0.0017	51.
5	0.46	3.26	0.0318	180.	0.0246	36	0.0017	51.
6	0.51	3.62	0.0353	185.	0.0267	37	0.0017	51.
7	0.45	3.49	0.0341	180.	0.0266	36	0.0018	51.
8	0.27	3.39	0.0337	190.	0.0284	38	0.0021	51.
9	0.39	3.35	0.0331	180.	0.0292	36	0.0021	51.
10	0.43	3.52	0.0347	175.	0.0306	35	0.0022	51.
11	0.40	3.39	0.0334	170.	0.0287	34	0.0023	51.
12	0.07	3.00	0.0300	160.	0.0259	32	0.0025	51.
13	0.09	2.91	0.0291	175.	0.0257	35	0.0026	51.
14	0.15	2.97	0.0297	180.	0.0267	36	0.0026	51.
15	0.35	3.29	0.0325	185.	0.0297	37	0.0026	51.
16	0.31	3.21	0.0318	185.	0.0292	37	0.0026	51.
17	0.28	3.25	0.0322	185.	0.0297	37	0.0025	51.
18	0.30	3.31	0.0329	185.	0.0303	37	0.0025	51.
19	0.25	3.41	0.0339	180.	0.0314	36	0.0024	51.

F(S) STANDARD DEVIATION ALL CASES = 0.0331 MEAN = 0.0027 DEGREES OF FREEDOM = 3415.

F(SA) STANDARD DEVIATION ALL CASES = 0.0272 MEAN = 0.0027 DEGREES OF FREEDOM = 683.

F(R) STANDARD DEVIATION ALL CASES = 0.0021 MEAN = 0.0000 DEGREES OF FREEDOM = 969.

TABLE 7 - CYCLE 7 F(S), F(SA) and F(R) Data. Original W¹, Reused Detectors Included.

SUMMARY EDIT FOR ALL CASES THIS RUN
CASE AVERAGE SEGMENT RMS SEGMENT
DEVIATION % DEVIATION

CASE	AVERAGE SEGMENT DEVIATION	RMS SEGMENT % DEVIATION	F(S) ST. DEV.	F(S) OBSERV.	F(SA) ST. DEV.	F(SA) OBSERV.	F(R) ST. DEV.	F(R) OBSERV.
1	0.18	2.89	0.0286	180.	0.0213	36	0.0014	51.
2	0.38	3.39	0.0332	185.	0.0242	37	0.0015	51.
3	0.28	3.61	0.0357	175.	0.0175	35	0.0018	51.
4	0.23	3.37	0.0332	180.	0.0208	36	0.0017	51.
5	0.33	3.00	0.0294	180.	0.0213	36	0.0017	51.
6	0.40	3.43	0.0335	185.	0.0240	37	0.0017	51.
7	0.33	3.25	0.0318	180.	0.0234	36	0.0018	51.
8	0.16	3.15	0.0315	190.	0.0257	38	0.0021	51.
9	0.28	3.11	0.0309	180.	0.0266	36	0.0021	51.
10	0.30	3.27	0.0324	175.	0.0279	35	0.0022	51.
11	0.28	3.14	0.0311	170.	0.0259	34	0.0023	51.
12	-0.07	2.64	0.0266	160.	0.0217	32	0.0025	51.
13	-0.05	2.55	0.0256	175.	0.0215	35	0.0026	51.
14	0.04	2.65	0.0266	180.	0.0232	36	0.0025	51.
15	0.24	3.01	0.0299	185.	0.0268	37	0.0026	51.
16	0.20	2.92	0.0291	185.	0.0262	37	0.0026	51.
17	0.17	2.95	0.0295	185.	0.0266	37	0.0025	51.
18	0.18	3.02	0.0301	185.	0.0273	37	0.0025	51.
19	0.13	3.12	0.0312	180.	0.0284	36	0.0024	51.

F(S) STANDARD DEVIATION ALL CASES = 0.0306 MEAN = 0.0016 DEGREES OF FREEDOM = 3415.

F(SA) STANDARD DEVIATION ALL CASES = 0.0241 MEAN = 0.0016 DEGREES OF FREEDOM = 683.

F(R) STANDARD DEVIATION ALL CASES = 0.0021 MEAN = 0.0000 DEGREES OF FREEDOM = 969.

TABLE 8 - CYCLE 7 F(s), F(sa), F(r) Data. New W', Reused Detectors Included.

SUMMARY EDIT FOR ALL CASES THIS RUN
CASE AVERAGE SEGMENT RMS SEGMENT
DEVIATION % DEVIATION

	F(S) ST. DEV.	F(S) OBSERV.	F(SA) ST. DEV.	F(SA) OBSERV.	F(R) ST. DEV.	F(R) OBSERV.		
1	0.53	2.33	0.0225	155.	0.0164	31	0.0014	51.
2	0.79	3.02	0.0285	160.	0.0202	32	0.0015	51.
3	0.34	3.31	0.0329	150.	0.0158	30	0.0018	51.
4	0.42	2.98	0.0292	155.	0.0169	31	0.0017	51.
5	0.60	2.48	0.0237	155.	0.0169	31	0.0017	51.
6	0.77	3.05	0.0288	160.	0.0200	32	0.0017	51.
7	0.73	2.83	0.0267	155.	0.0194	31	0.0018	51.
8	0.68	2.82	0.0269	165.	0.0208	33	0.0021	51.
9	0.88	2.80	0.0261	155.	0.0211	31	0.0021	51.
10	0.95	2.95	0.0274	150.	0.0219	30	0.0022	51.
11	0.75	2.86	0.0270	150.	0.0212	30	0.0023	51.
12	0.39	2.24	0.0219	140.	0.0161	28	0.0025	51.
13	0.39	2.14	0.0208	155.	0.0162	31	0.0026	51.
14	0.50	2.25	0.0216	160.	0.0178	32	0.0025	51.
15	0.74	2.69	0.0253	165.	0.0220	33	0.0025	51.
16	0.70	2.58	0.0245	165.	0.0213	33	0.0026	51.
17	0.69	2.61	0.0248	165.	0.0217	33	0.0025	51.
18	0.72	2.68	0.0254	165.	0.0223	33	0.0025	51.
19	0.72	2.74	0.0260	160.	0.0228	32	0.0024	51.

F(S) STANDARD DEVIATION ALL CASES = 0.0259 MEAN = 0.0061 DEGREES OF FREEDOM = 2985.

F(SA) STANDARD DEVIATION ALL CASES = 0.0195 MEAN = 0.0062 DEGREES OF FREEDOM = 597.

F(R) STANDARD DEVIATION ALL CASES = 0.0021 MEAN = 0.0000 DEGREES OF FREEDOM = 969.

TABLE 9- CYCLE 7 F(s), F(sa) and F(r) Data. Omitted Reused Detectors, New W

SUMMARY EDIT FOR ALL CASES THIS RUN
CASE AVERAGE SEGMENT RMS SEGMENT
DEVIATION % DEVIATION

			F(S) ST. DEV.	F(S) OBSERV.	F(SA) ST. DEV.	F(SA) OBSERV.	F(R) ST. DEV.	F(R) OBSERV.
1	0.44	3.30	0.0324	195.	0.0216	39	0.0021	51.
2	0.38	2.61	0.0259	190.	0.0200	38	0.0021	51.
3	0.33	2.56	0.0254	195.	0.0199	39	0.0018	51.
4	0.32	2.66	0.0264	190.	0.0208	38	0.0018	51.
5	0.22	3.60	0.0356	169.	0.0256	33	0.0023	51.
6	0.24	2.81	0.0282	165.	0.0210	33	0.0024	51.
7	0.19	3.09	0.0314	164.	0.0253	32	0.0024	51.
8	0.19	2.67	0.0266	177.	0.0227	35	0.0024	51.
9	0.21	2.94	0.0295	177.	0.0258	35	0.0023	51.
10	0.11	2.66	0.0268	177.	0.0229	35	0.0025	51.
11	0.11	2.74	0.0271	177.	0.0227	35	0.0026	51.
12	0.14	2.93	0.0293	167.	0.0251	33	0.0026	51.
13	0.24	2.76	0.0275	158.	0.0228	31	0.0026	51.
14	0.17	3.23	0.0311	152.	0.0251	30	0.0024	51.
15	-0.05	3.26	0.0324	148.	0.0270	29	0.0023	51.
16	-0.01	2.80	0.0280	160.	0.0239	32	0.0022	51.
17	-0.05	3.41	0.0341	172.	0.0280	34	0.0021	51.
18	-0.01	2.94	0.0291	161.	0.0255	32	0.0021	51.
19	0.04	3.29	0.0336	152.	0.0182	30	0.0017	51.
20	0.01	3.09	0.0314	163.	0.0149	32	0.0018	51.
21	0.00	2.90	0.0294	168.	0.0130	33	0.0015	51.
22	-0.03	3.06	0.0314	175.	0.0136	35	0.0016	51.
23	-0.01	2.94	0.0299	175.	0.0134	35	0.0020	51.
24	-0.08	2.67	0.0267	170.	0.0114	34	0.0022	51.
25	-0.15	2.38	0.0238	155.	0.0114	31	0.0022	51.
26	-0.15	2.37	0.0236	160.	0.0110	32	0.0023	51.
27	-0.10	2.42	0.0242	160.	0.0114	32	0.0023	51.
28	-0.14	2.29	0.0228	160.	0.0108	32	0.0024	51.
29	-0.17	2.28	0.0226	155.	0.0107	31	0.0023	51.
30	-0.15	2.22	0.0221	155.	0.0106	31	0.0026	51.
31	-0.23	2.79	0.0283	145.	0.0123	29	0.0026	51.
32	-0.06	3.13	0.0318	140.	0.0130	28	0.0028	51.
33	-0.15	2.97	0.0306	152.	0.0132	30	0.0028	51.
34	-0.18	2.34	0.0241	152.	0.0124	30	0.0025	51.
35	-0.23	2.37	0.0244	152.	0.0126	30	0.0026	51.
36	0.53	2.33	0.0225	155.	0.0164	31	0.0014	51.
37	0.79	3.02	0.0285	160.	0.0202	32	0.0015	51.
38	0.34	3.31	0.0329	150.	0.0158	30	0.0018	51.
39	0.42	2.98	0.0292	155.	0.0169	31	0.0017	51.
40	0.60	2.48	0.0237	155.	0.0169	31	0.0017	51.
41	0.77	3.05	0.0288	160.	0.0200	32	0.0017	51.
42	0.73	2.83	0.0267	155.	0.0194	31	0.0018	51.
43	0.68	2.82	0.0269	165.	0.0208	33	0.0021	51.
44	0.88	2.80	0.0261	155.	0.0211	31	0.0021	51.
45	0.95	2.95	0.0274	150.	0.0219	30	0.0022	51.
46	0.75	2.86	0.0270	150.	0.0212	30	0.0023	51.
47	0.39	2.24	0.0219	140.	0.0161	28	0.0025	51.
48	0.39	2.14	0.0208	155.	0.0162	31	0.0026	51.
49	0.50	2.25	0.0216	160.	0.0178	32	0.0025	51.
50	0.74	2.69	0.0253	165.	0.0220	33	0.0026	51.
51	0.70	2.58	0.0245	165.	0.0213	33	0.0026	51.
52	0.69	2.61	0.0248	165.	0.0217	33	0.0025	51.
53	0.72	2.68	0.0254	165.	0.0223	33	0.0025	51.
54	0.72	2.74	0.0260	160.	0.0228	32	0.0024	51.

F(S) STANDARD DEVIATION ALL CASES = 0.0277 MEAN = 0.0022 DEGREES OF FREEDOM = 8768. ✓
F(SA) STANDARD DEVIATION ALL CASES = 0.0194 MEAN = 0.0022 DEGREES OF FREEDOM = 1754. ✓
F(R) STANDARD DEVIATION ALL CASES = 0.0022 MEAN = 0.0000 DEGREES OF FREEDOM = 2754. ✓

TABLE 10 - CYCLES 5,6,7 Data Combined. No reused detector data for cycle

SUMMARY EDIT FOR ALL CASES THIS RUN
 CASE F(Z) F(Z) BLOCK
 ST. DEV. OBSERV.

COMPUTER
 RUN DATE

POWER
 SPLIT

CASE	F(Z) ST. DEV.	F(Z) OBSERV.	BLOCK	COMPUTER RUN DATE	POWER SPLIT
1	0.0168	51.	173	890331 120151200	-0.3997
2	0.0169	51.	175	890331 120713400	-0.3265
3	0.0162	51.	176	890331 122518910	-0.2758
4	0.0150	51.	177	890331 122839300	-0.2140
5	0.0140	51.	178	890331 123233500	-0.1386
6	0.0135	51.	179	890331 123541400	-0.0514
7	0.0117	51.	180	890331 123903800	0.0452
8	0.0150	51.	181	890331 124307900	0.1435
9	0.0119	51.	182	890331 124540200	0.2341
10	0.0131	51.	183	890331 124901700	0.3047
11	0.0137	51.	186	890331 130048600	0.3921
12	0.0023	51.	5	890403 111937710	-0.0181
13	0.0016	51.	21	890403 113038680	-0.0071
14	0.0020	51.	26	890403 113746680	0.0011
15	0.0038	51.	34	890403 114504490	-0.0006
16	0.0060	51.	50	890403 122824420	0.0144
17	0.0108	51.	67	890403 123356290	0.0250
18	0.0144	51.	97	890403 123929710	0.0377
19	0.0167	51.	120	890403 124447390	0.0399
20	0.0178	51.	139	890403 125013590	-0.1834
21	0.0174	51.	149	890403 130227920	0.0346
22	0.0149	51.	162	890403 131014030	0.0319

F(Z) STANDARD DEVIATION ALL CASES = 0.0151 MEAN = 0.0086 DEGREES OF FREEDOM = 1122.

TABLE 11 - CYCLE 7 F(Z) Data

TABLES

Statistical Variable	Standard Deviation	Degrees of Freedom	Tolerance Factor	Tolerance Limit
F(s) #	0.0393	1800	--	--
F(sa)#	0.0351	360	--	--
F(r) #	0.0026	408	--	--
F(s) *	0.0306	3415	--	--
F(sa)*	0.0241	683	--	--
F(r) *	0.0021	969	--	--
F(s)	0.0277	8768	--	--
F(sa)	0.0194	1754	--	--
F(r)	0.0022	2754	--	--
F(z)	0.0151	1122	--	--
F(L)	0.0135	188	--	--
F(q) #	0.0433	2487	1.703	0.0795
F(Δ h)#	0.0383	489	1.766	0.0722
F(Ar)#	0.0352	364	1.785	0.0695
F(q) *	0.0368	3822	1.692	0.0664
F(Δ h)*	0.0277	877	1.733	0.0526
F(Ar)*	0.0242	694	1.746	0.0490
F(q)	0.0344	4826	1.692	0.0623
F(Δ h)	0.0237	1225	1.727	0.0455
F(Ar)	0.0195	1790	1.712	0.0401

#--values for cores when quadrant power tilt exceeds 2.8% but is less than or equal to 5%.

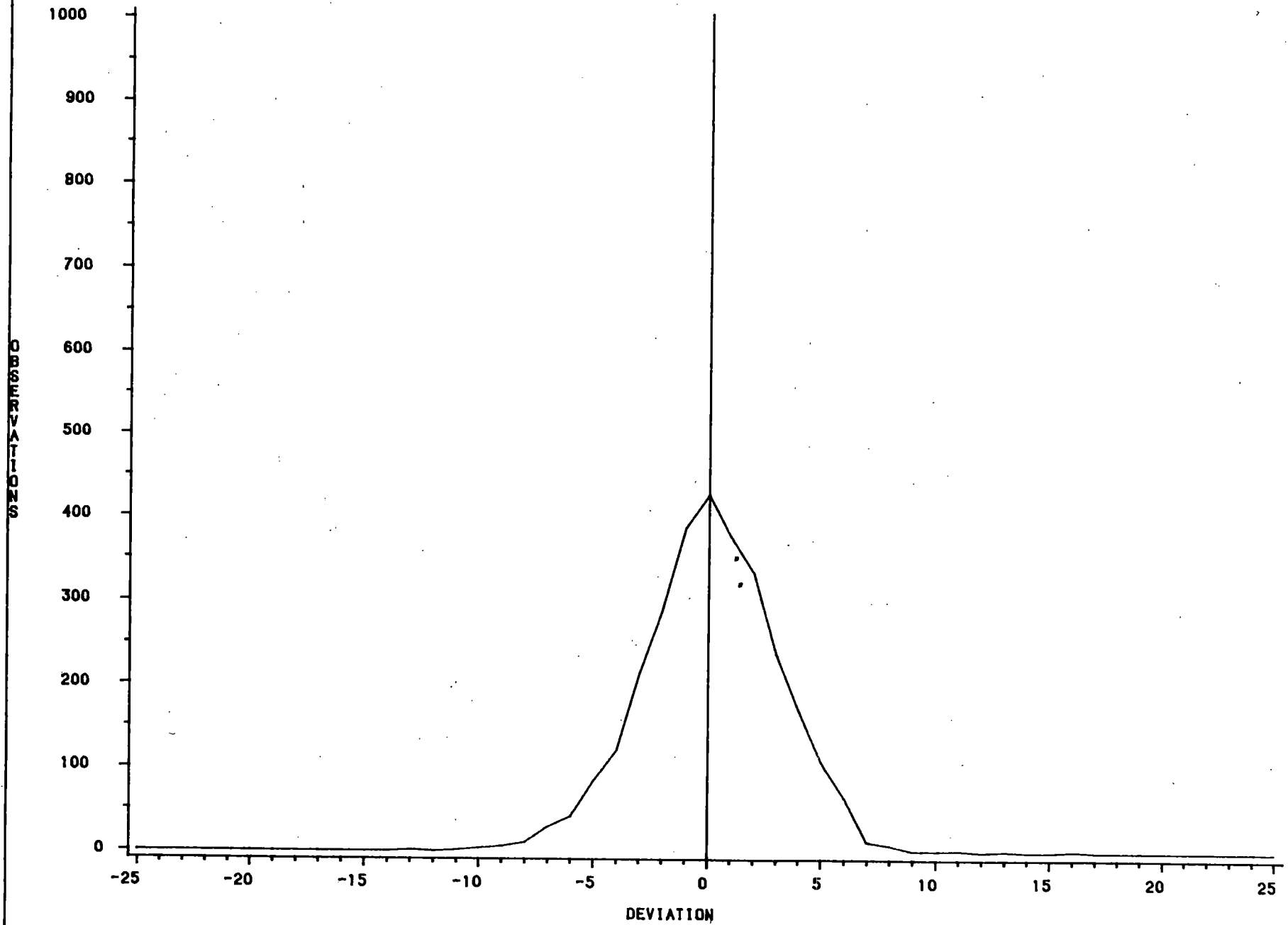
*--values for cores with once-burned reused incore detectors

For the final tolerance limits, penalty factors of .0041, .0046 and .0067 for F(q), F(Δ h) and F(Ar) respectively were included to account for up to 25% incore detector failures.

Table #12--Summary of statistical component uncertainties.

0986 1730

CYCLE 5 FULL CORE F (s) SYNTHESIS % DEVIATIONS

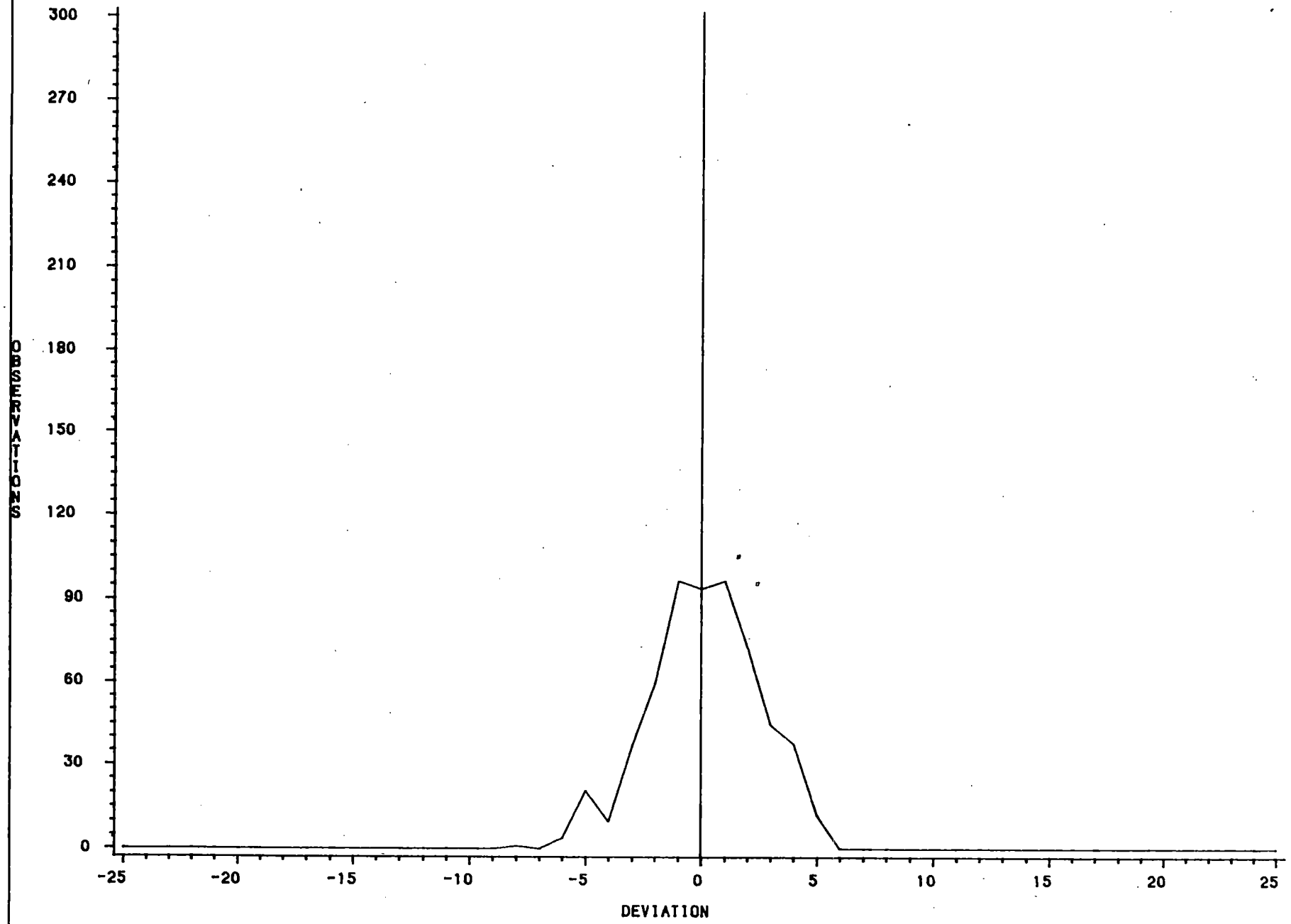


G.A. BAUSTIAN

26APR89

FIGURE #1

CYCLE 5 FULL CORE F(s_a) SYNTHESIS % DEVIATIONS



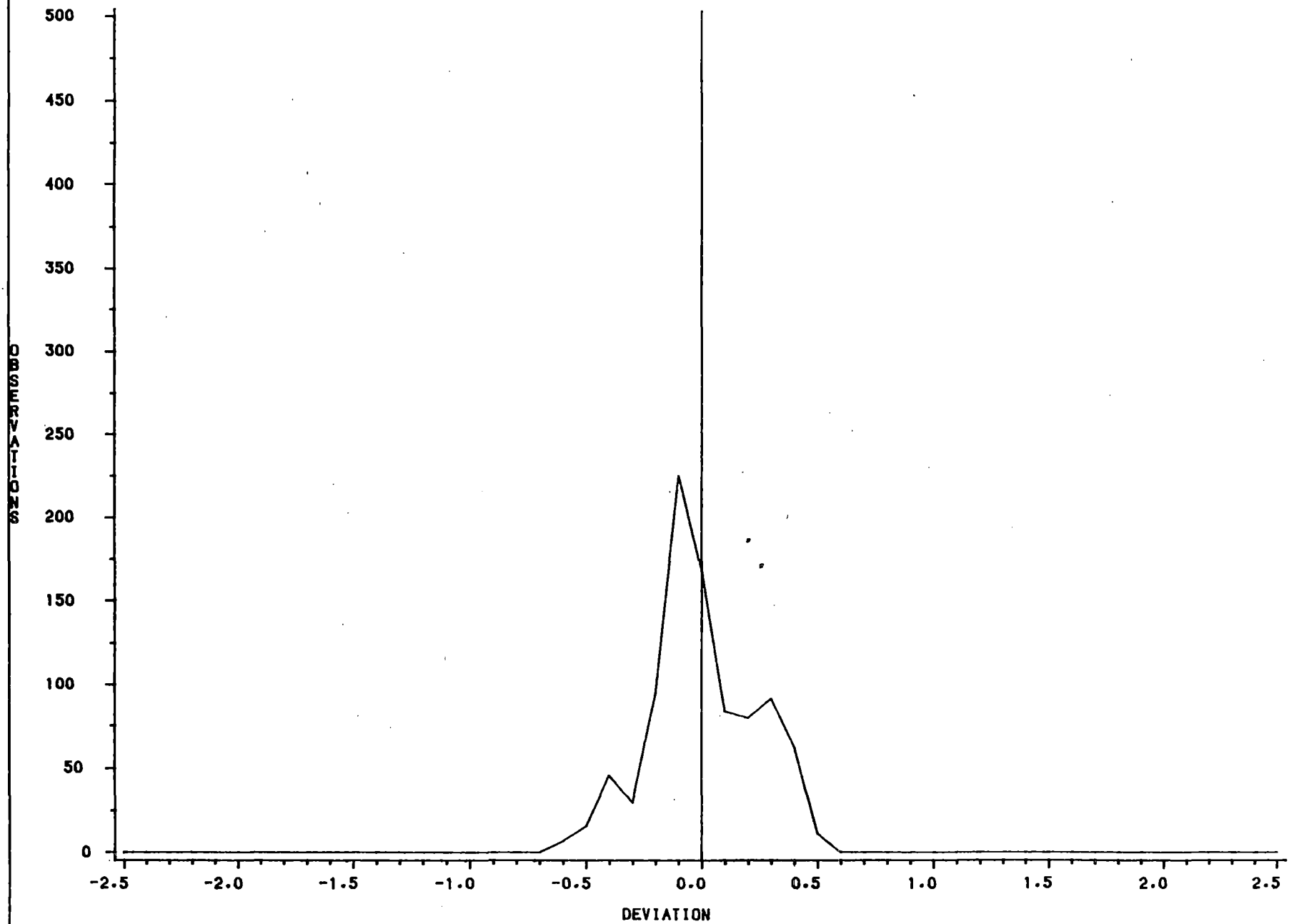
G.A. BAUSTIAN

26APR89

FIGURE #2

P32 REV 2

CYCLE 5 FULL CORE F(r) SYNTHESIS % DEVIATIONS

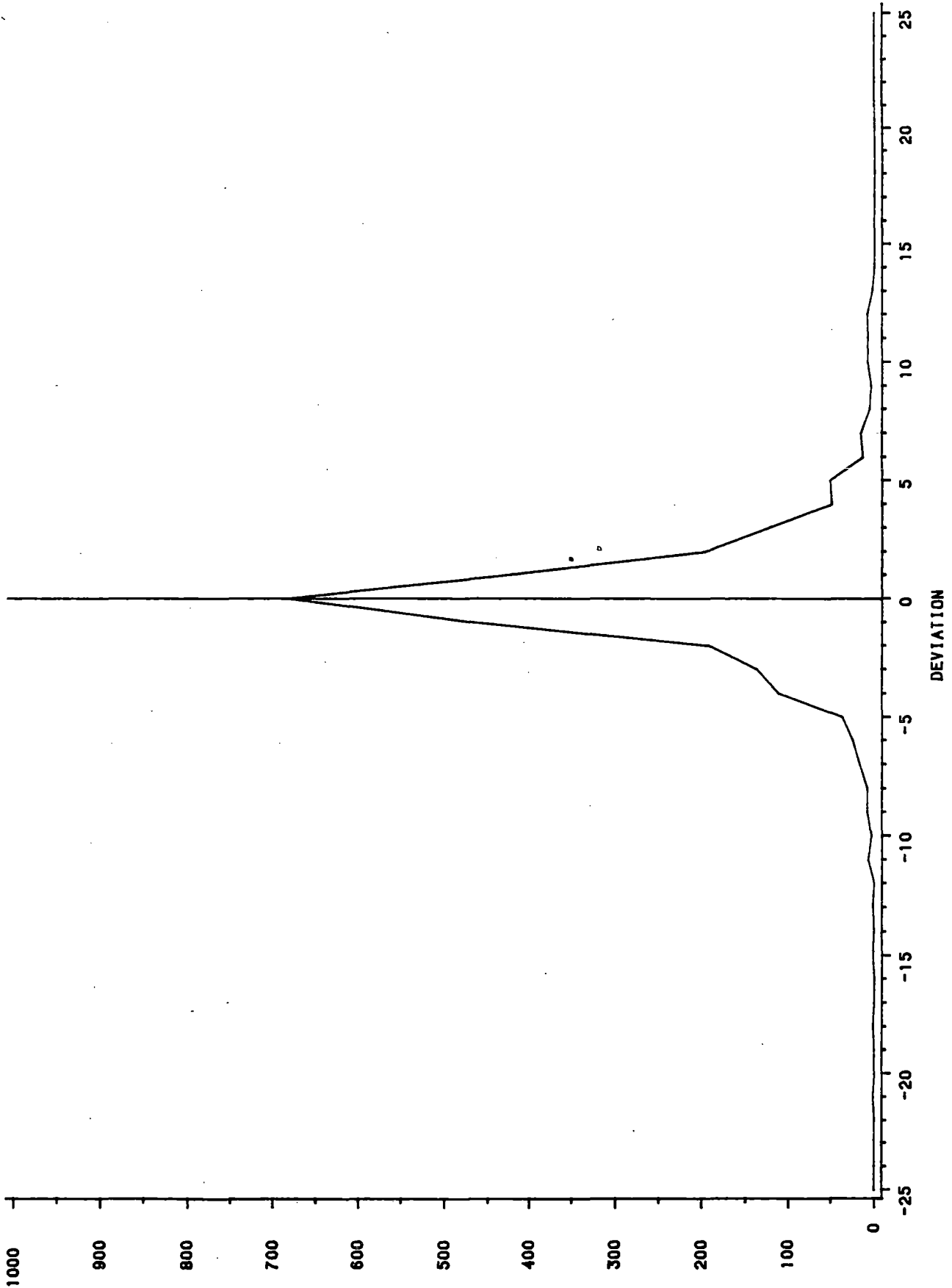


G.A. BAUSTIAN

26APR89

Figure #3

CYCLE 6 FULL CORE F(s) SYNTHESIS % DEVIATIONS

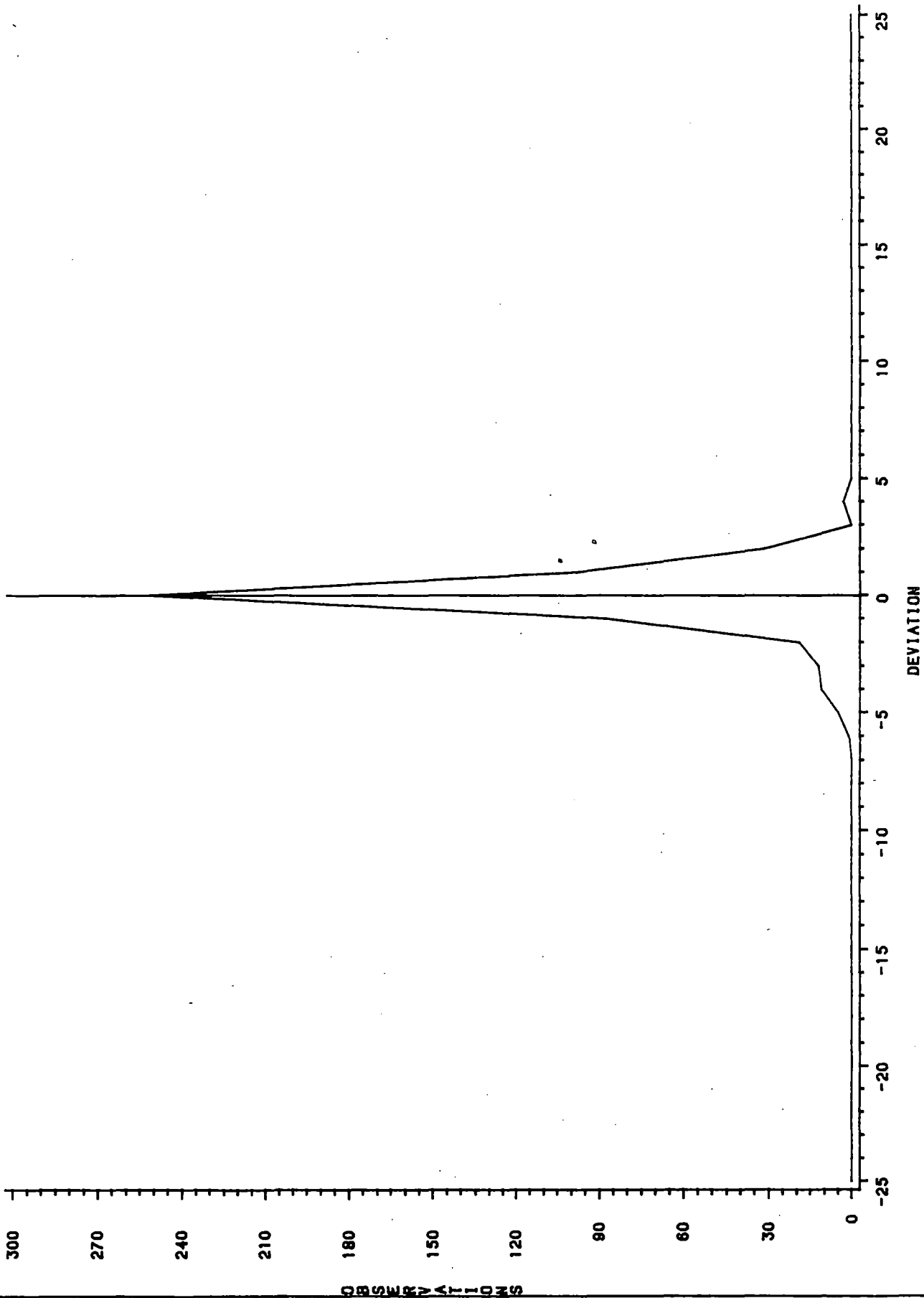


26APR89

G.A. BAUSTIAN

Figure #4

CYCLE 6 FULL CORE F(9a) SYNTHESIS % DEVIATIONS

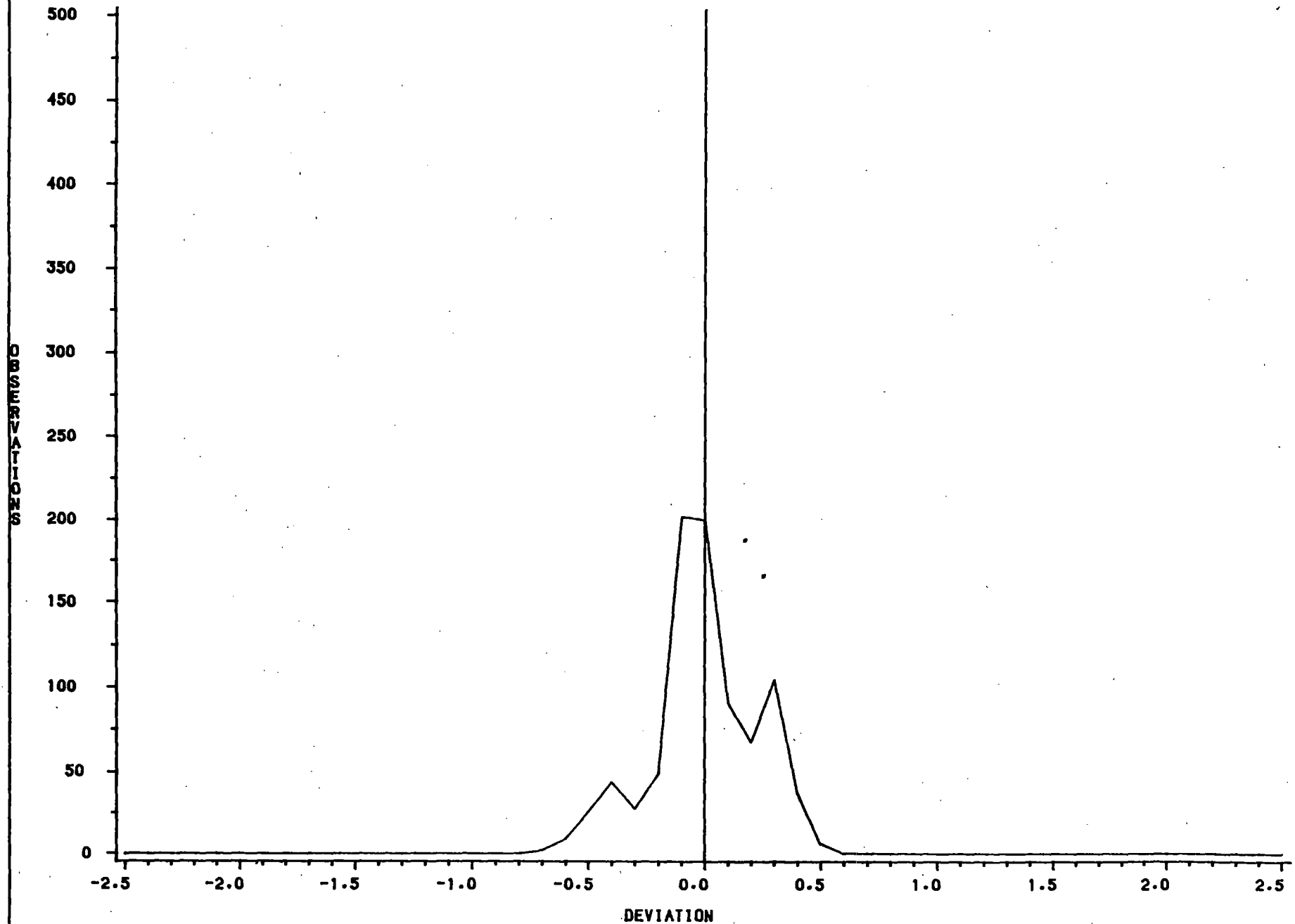


26 APR 89

G.A. BAUSTIAN

Figure #5

CYCLE 6 FULL CORE F(r) SYNTHESIS % DEVIATIONS



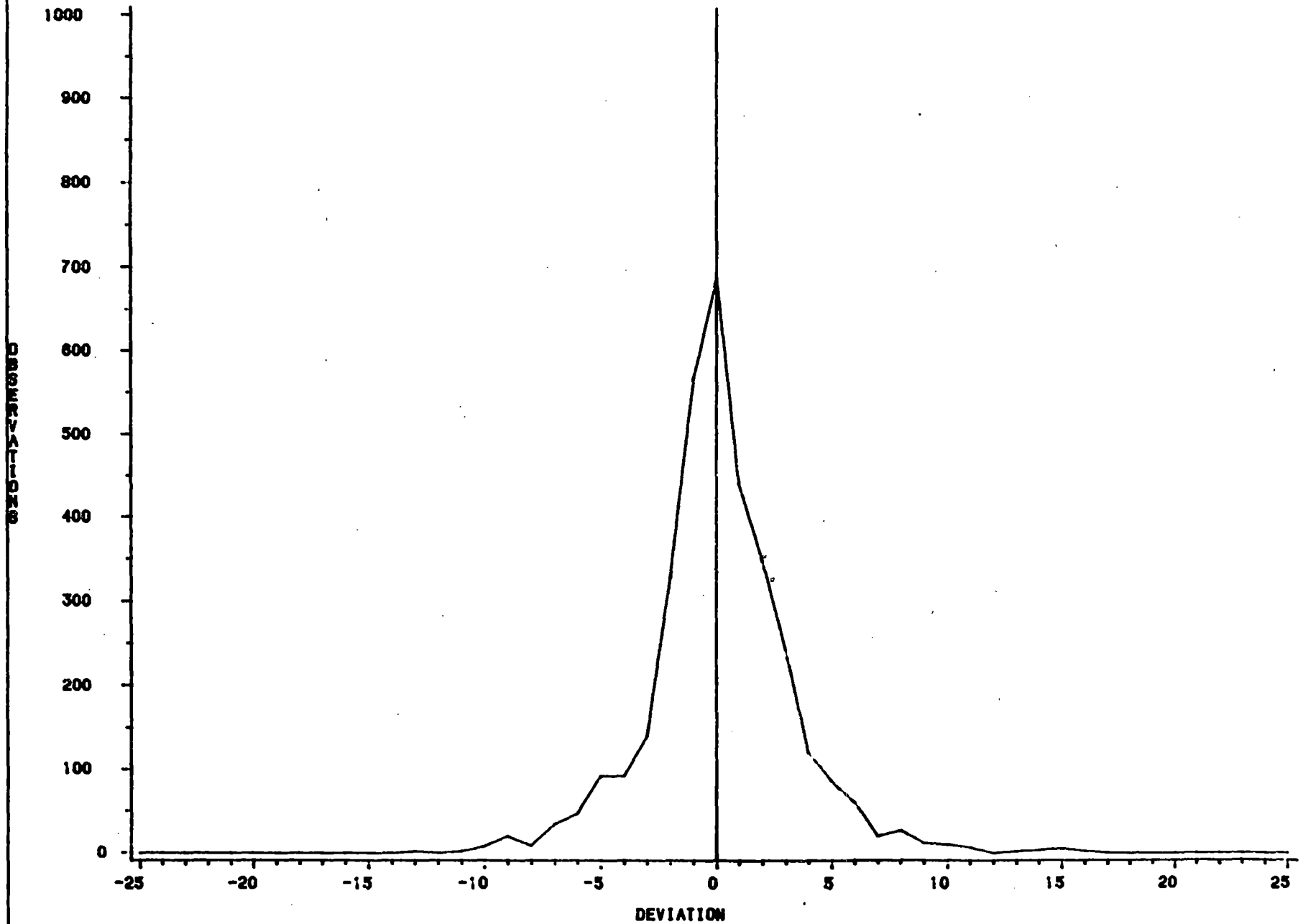
G.A. BAUSTIAN

26APR89

Figure #16

P36 REV 2

CYCLE 7 FULL CORE F(9) SYNTHESIS % DEVIATIONS, INCLUDING REUSED DETECTORS



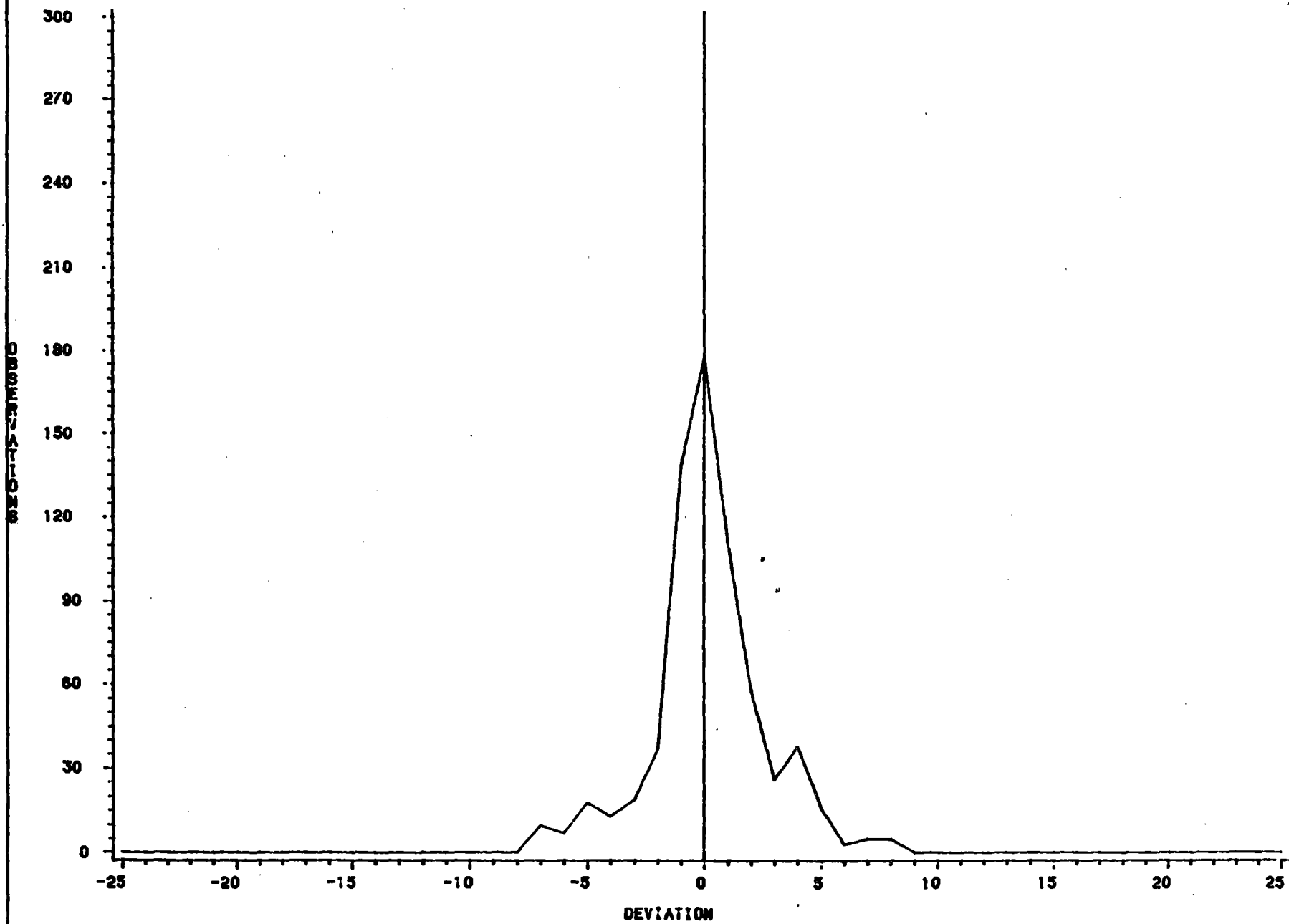
B.A. BAUSTIAN

4APR89

Figure #7

P37 REV 2

CYCLE 7 FULL CORE F(%) SYNTHESIS% DEVIATIONS, INCLUDING REUSED DETECTORS

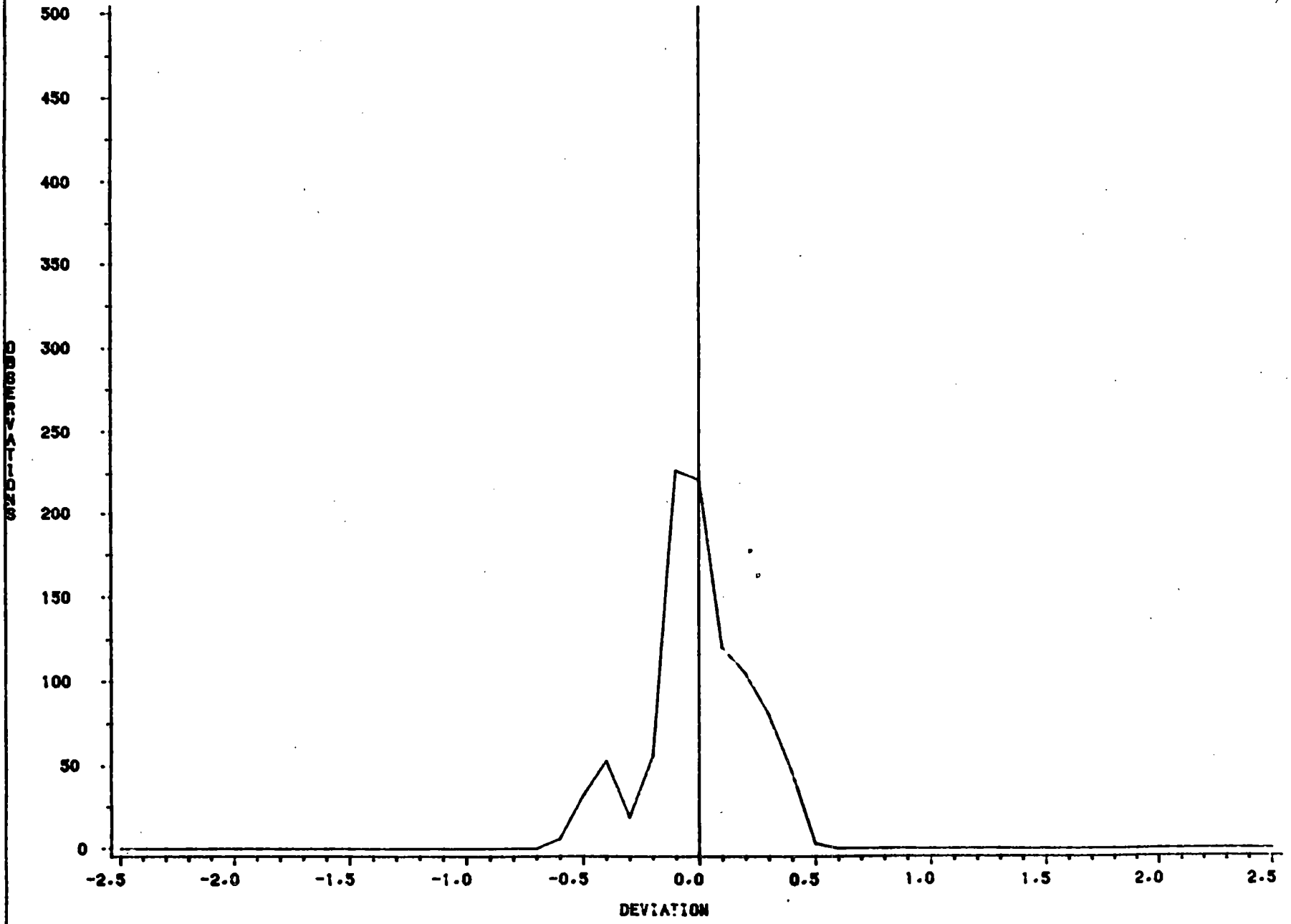


B.A. BAUSTIAN

4APR69

Figure #8

CYCLE 7 FULL CORE F (r) SYNTHESIS % DEVIATIONS, INCLUDING REUSED DETECTORS



G.A. BAUSTIAN

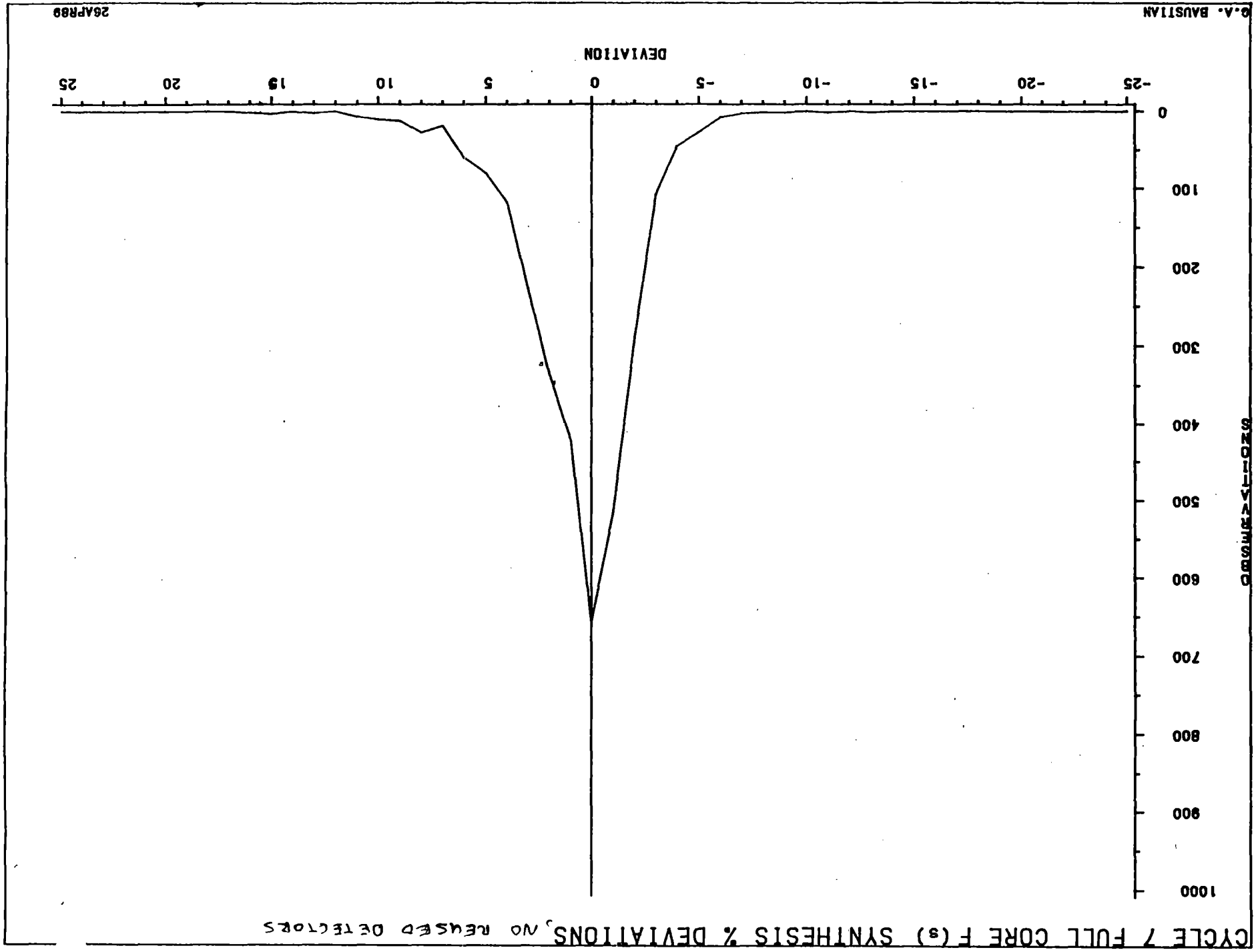
4 APR 69

Figure #9

P39 REV 2

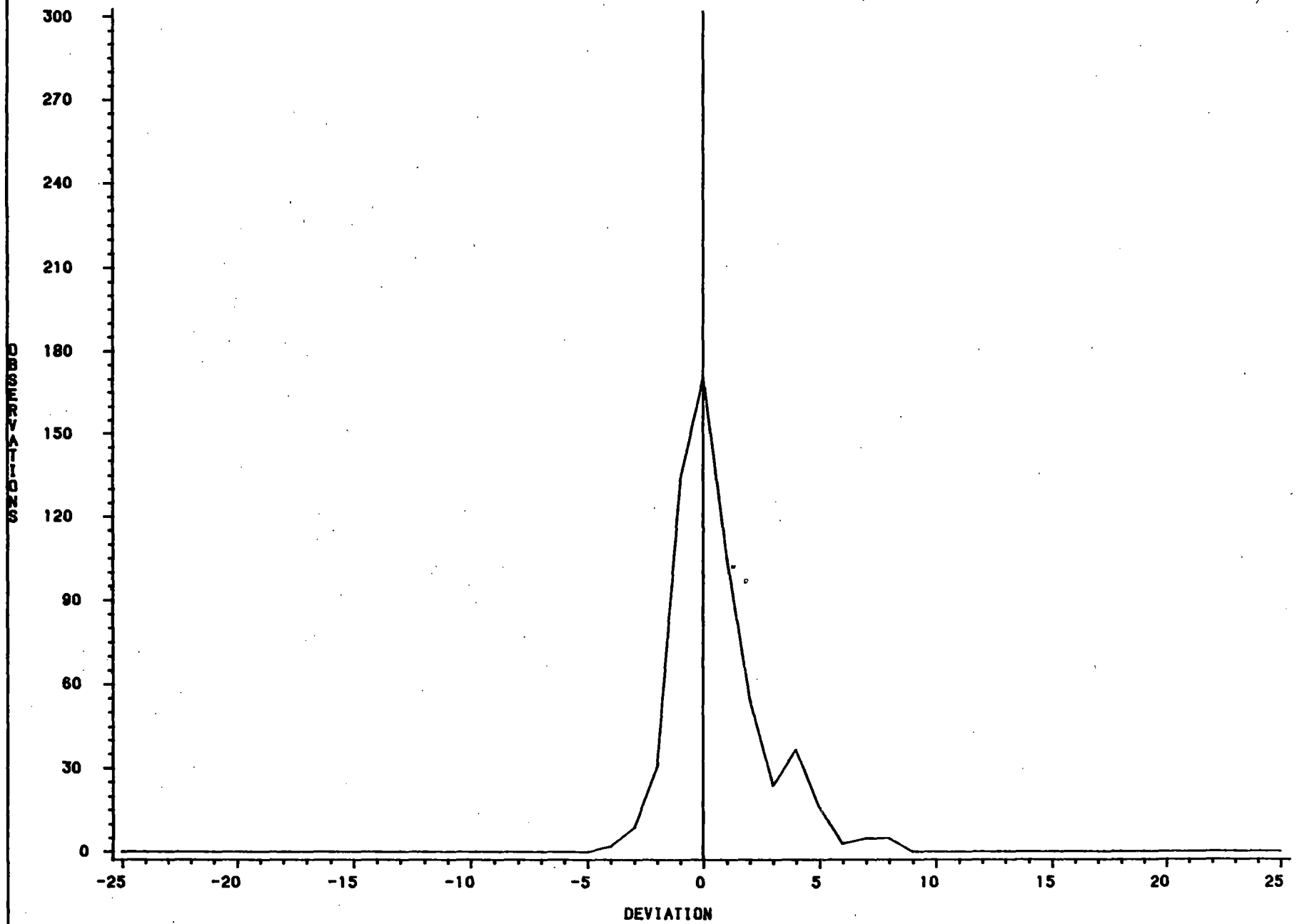
Figure #10

P40 REV 2



CYCLE 7 FULL CORE F (S) SYNTHESIS % DEVIATIONS, NO REASED DETECTORS

CYCLE 7 FULL CORE F (sa) SYNTHESIS % DEVIATIONS, NO REUSED DETECTORS



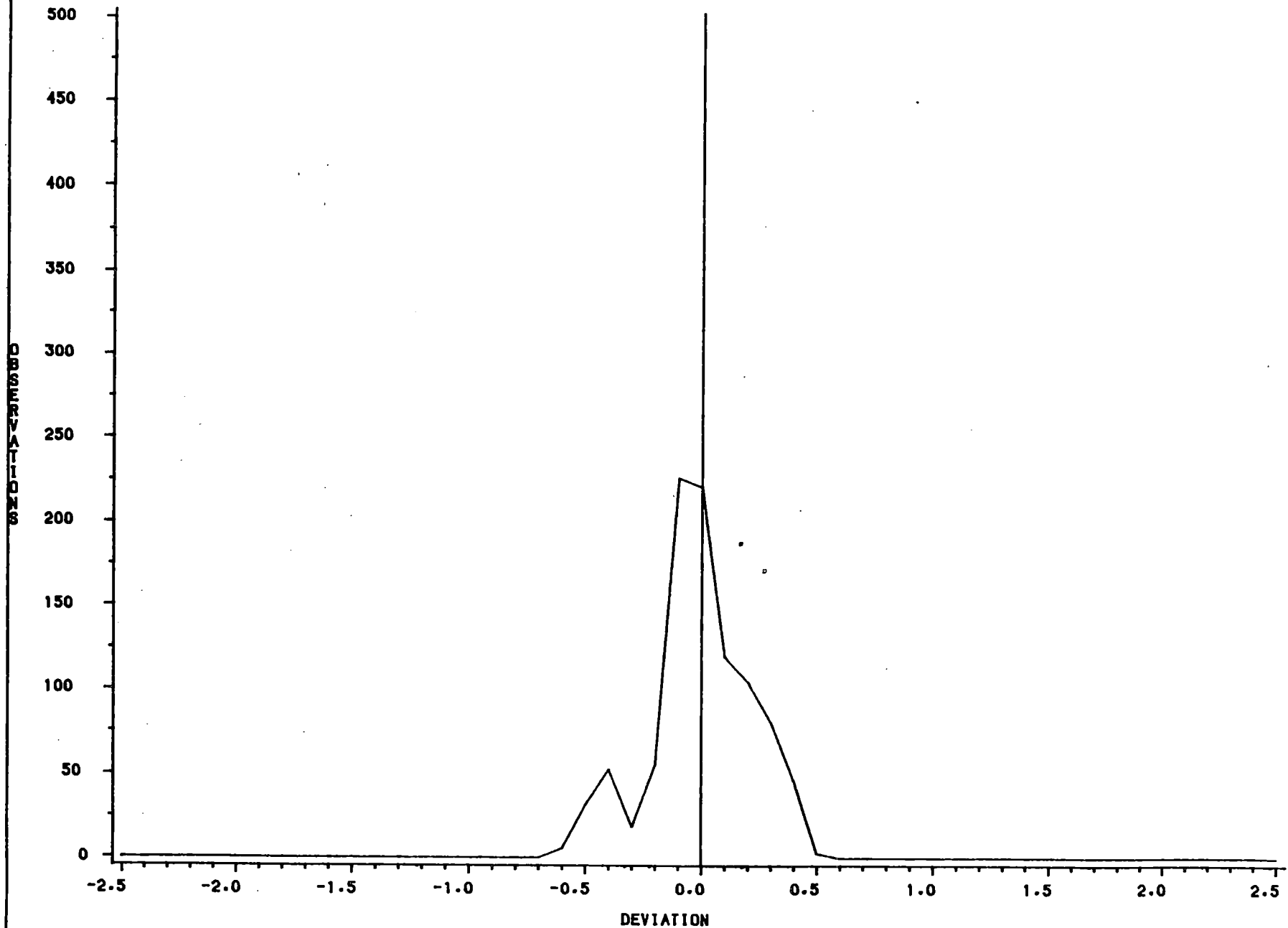
G.A. BAUSTIAN

26APR89

Figure #11

P41 REV 2

CYCLE 7 FULL CORE F (r) SYNTHESIS % DEVIATIONS, NO REUSED DETECTORS



G.A. BAUSTIAN

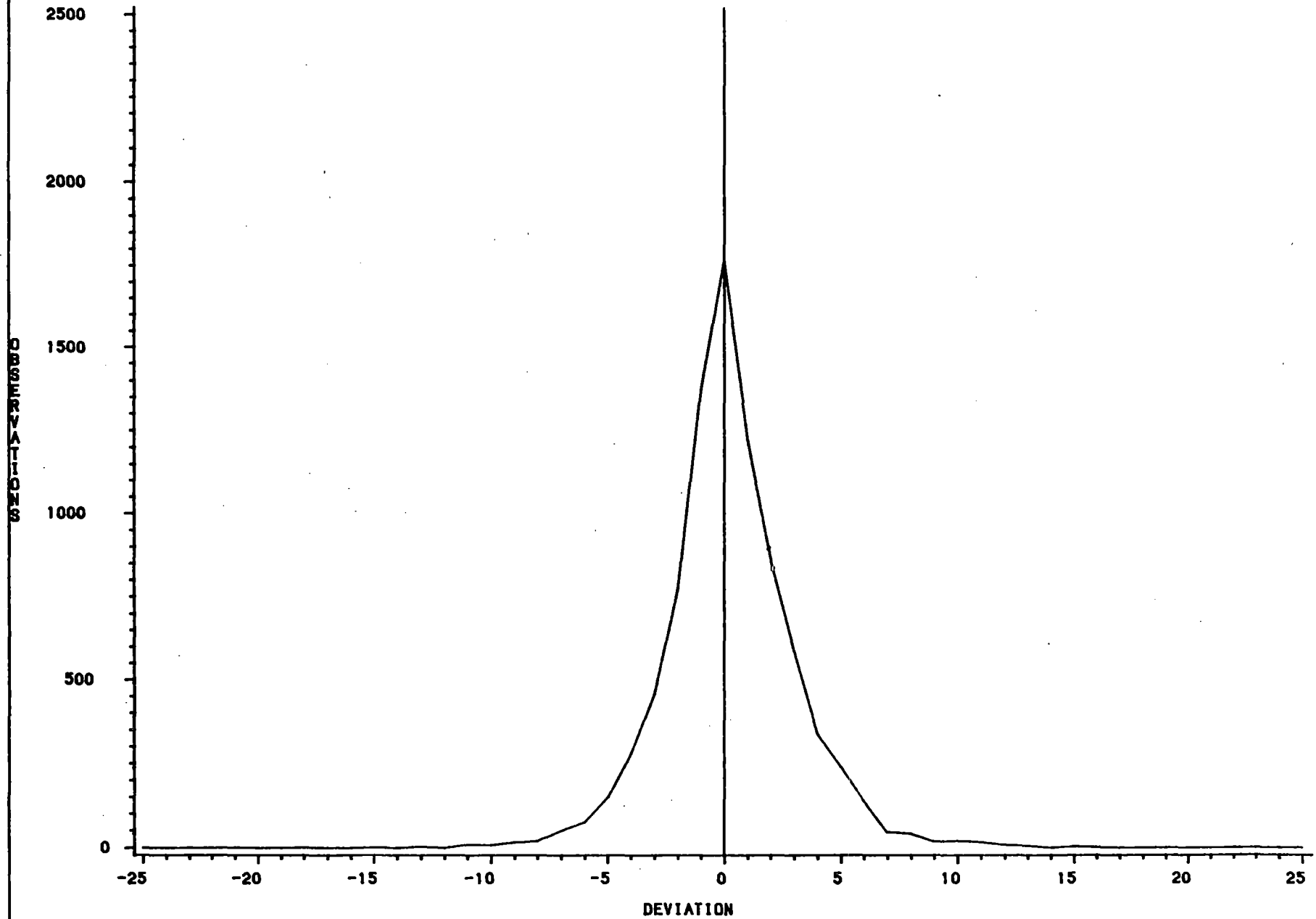
26APR89

Figure #12

P42 REV 2

FULL CORE F(s) SYNTHESIS % DEVIATIONS

Cycles 5, 6 and 7

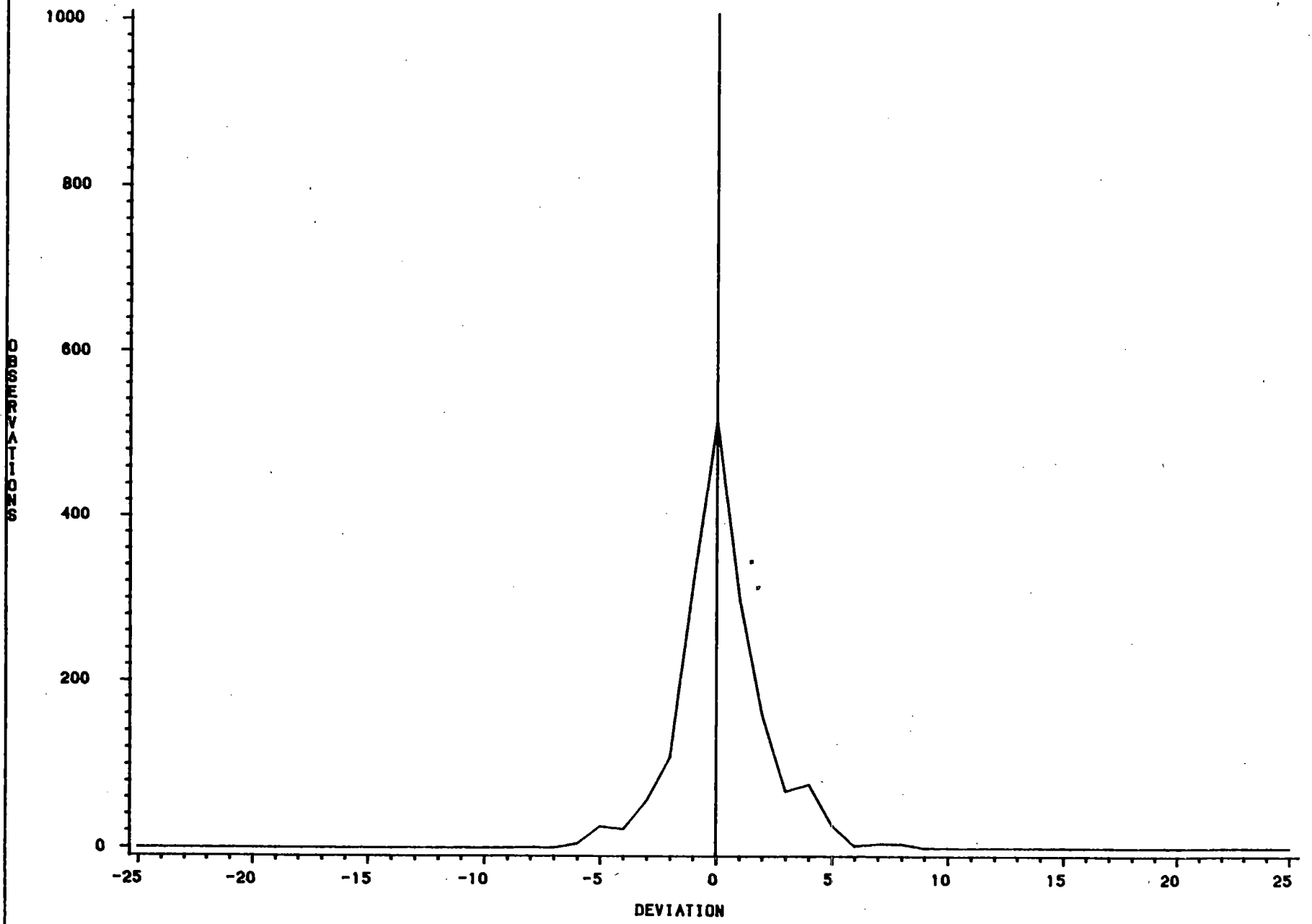


C.A. BAUSTIAN

26APR89

Figure #13

FULL CORE F (sa) SYNTHESIS % DEVIATIONS
Cycles 5, 6 and 7



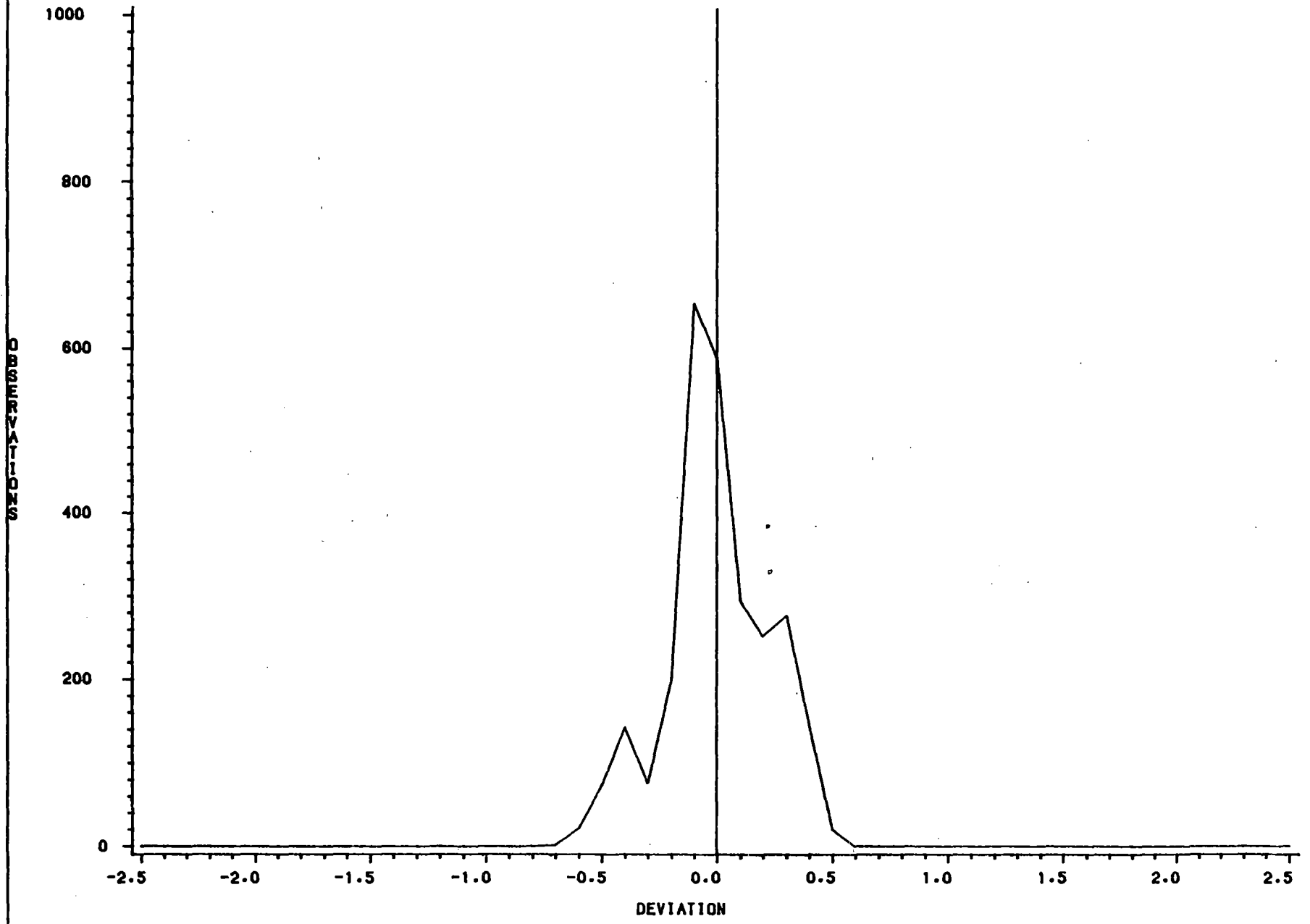
G.A. BAUSTIAN

26APR89

Figure #14

P44
REV 2

FULL CORE F(r) SYNTHESIS % DEVIATIONS
Cycles 5, 6 and 7



G.A. BAUSTIAN

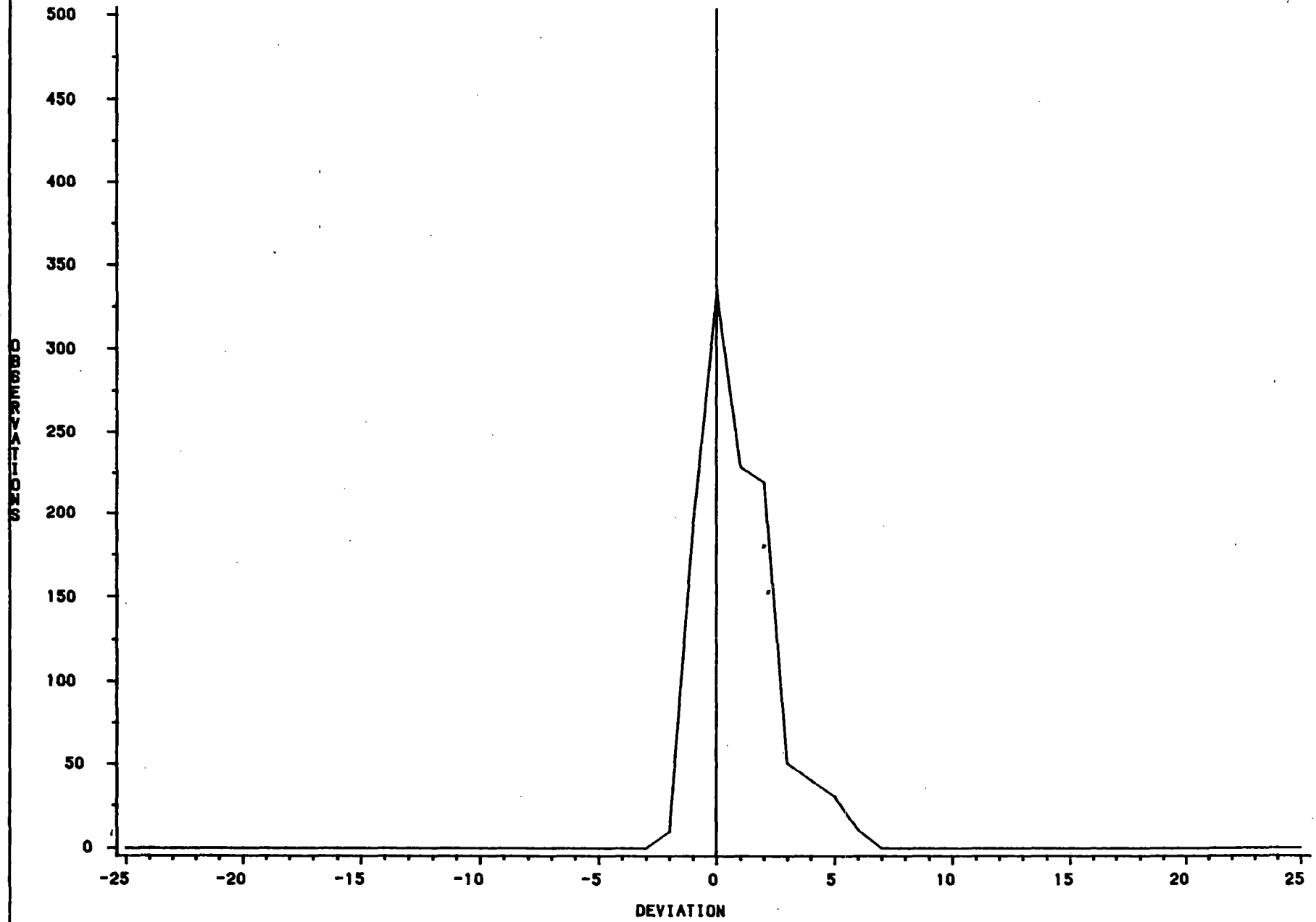
26APR89

Figure #15

P45
REV 2

FULL CORE F(z) SYNTHESIS % DEVIATIONS

Based on Cycle 7 Data



G.A. BAUSTIAN

26APR89

Figure #16

List of References

- | Number | Title |
|--------|--|
| 1 | P*PID*89001, The Palisades Full Core PIDAL System Methodology and Programmers Manual by GA Baustian, Consumers Power Company, Palisades Reactor Engineering |
| 2 | XN-NF-83-01(P), Exxon Nuclear Analysis of Power Distribution Measurement Uncertainty for St. Lucie Unit 1, January 1983. |
| 3 | Probability and Statistics for Engineers and Scientists, 2 Ed., RE Walpole and RH Myers, Macmillan Publishing Co, 1978. |
| 4 | Factors for One-Sided Tolerance Limits and for Variable Sampling Plans, D.B. Owen, Sandia Corporation Monograph, SCR-607, March 1963. |
| 5 | Radiation Detection and Measurement, Glenn F. Knoll, Wiley Publishing Co, 1979. |
| 6 | CALCULATIONAL VERIFICATION OF THE COMBUSTION ENGINEERING FULL CORE INSTRUMENTATION ANALYSIS SYSTEM CECOR, W.B. TERNEY et al, Combustion Engineering, presented at International Conference On World Nuclear Power, Washington D.C., November 19, 1976. |
| 7 | Palisades Reactor Engineering Dept. Benchmarking Calculation File For Fuel Cycles 5,6 and 7. |
| 8 | EA*GAB*90*06, PIDAL Quadrant Power Tilt Uncertainty, by GA Baustian, Consumers Power Company, Palisades Reactor Engineering. |

1781

0936

GLOSSARY

- INCA - An incore analysis program developed by Combustion Engineering to determine (measure) the power distribution within the Palisades reactor assuming one-eighth or octant core symmetry.
- PIDAL - An incore analysis program developed by Consumers Power Company to determine (measure) the power distribution within the Palisades on a full core basis.
- XTG - A group and one-half nodal diffusion theory code developed by Advanced Nuclear Fuels Corporation (formerly Exxon Nuclear) for general predictive modeling of pressurized water reactors.
- PDQ - A multi-group diffusion theory code, run primarily in two dimensions, capable of modeling each fuel pin in the reactor explicitly.
- CECOR - An incore analysis program developed by Combustion Engineering to determine (measure) the power distribution within a pressurized water reactor on a full core basis.
- Wprime - Factor used in conversion of measured incore detector millivolt signals to detector segment powers. Data supplied by ANF.
- Normal - Refers to a statistically "normal" or Gaussian distribution of data.
- 95/95 Tolerance Limit - this limit ensures that there is a 95 percent probability that at least 95 percent of the true peaking values will be less than the PIDAL measured/inferred peaking values plus the associated tolerance limit.

ATTACHMENT 2

Consumers Power Company
Palisades Plant
Docket 50-255

PIDAL
ANALYSIS OF QUADRANT POWER TILT UNCERTAINTIES

June 25, 1991

PALISADES INCORE DETECTOR ALGORITHM (PIDAL)
ANALYSIS OF QUADRANT POWER TILT UNCERTAINTIES

G.A. Baustian
Consumers Power Company

August 14,1990

CONTENTS

- 1: Objective
- 2: Summary of Results
- 3: Assumptions
- 4: Analysis Methodology
- 5: Analysis Results
- 6: Palisades Core Map

Objective

The purpose of the work described by this analysis was to determine the accuracy of the full core PIDAL power distribution calculations when the true core power distribution is radially tilted. This is in response to comments made by the USNRC while reviewing the PIDAL methodology and uncertainty analysis.

In particular, the NRC requested the following:

- 1 - A comparison of the tilt measured by PIDAL with the true or theoretical tilt.
- 2 - Verification that the PIDAL code programming was correct by supplying theoretical detector input and comparing the resulting PIDAL solution with the original theoretical power distribution solution.
- 3 - Determination of the $S_{F(s)}$ uncertainty component for radially perturbed or tilted power distributions up to the full power Technical Specification limit of 5% quadrant power tilt.
- 4 - An explanation of what assumptions are made in the Palisades Safety Analysis to cover radial peaking factor increases caused by quadrant power tilts.

Summary and Conclusions

Comparisons between the quadrant power tilts determined by the PIDAL model were made to corresponding theoretical values. It was found that in all cases PIDAL either accurately measured the quadrant power tilt, or in some instances conservatively measured the tilts to be greater than truth.

The $S_{F(s)}$ uncertainty component as defined in the PIDAL uncertainty analysis was recalculated for radially tilted cores. It was found that in all cases the $S_{F(s)}$ value for tilted cores was bounded by the value used in the PIDAL uncertainty analysis for cores with quadrant power tilts up to 2.8%. It was also found that the value of the $S_{F(s)}$ uncertainty component depended strongly on the direction and magnitude of the oscillation causing the power tilt. For cores oscillating about the diagonal core axis, the assumed PIDAL measurement uncertainty is valid for tilts up to 5%.

For the oscillation about the core major axis, the $S_{F(s)}$ uncertainty component ceases to be bounded by the value assumed in the PIDAL uncertainty analysis for quadrant power tilts greater than 2.8%. Since the Palisades Technical Specifications allow for full power operation with quadrant power tilts of up to 5%, and it was clear that the current PIDAL uncertainties were only valid for tilts up to 2.8%, it was necessary to derive new uncertainties to allow use of PIDAL for tilts above 2.8%. An analysis was performed, as described in Sections 3 and 4 of this report in order to determine the uncertainties in F_r^q , $F_r^{A_h}$ and F_r^A at the 5% quadrant power tilt threshold. These uncertainties may be found in Table #3 of Section 5 of this report.

It was shown that the coding in the PIDAL program is correct by reproducing a theoretically flat power distribution when given the appropriate theoretical incore detector values. This is in agreement with results previously obtained as part of the PIDAL Uncertainty Analysis.

Finally, it was found that quadrant power tilt is not an input to the Safety Analysis and that the increase in local or radial peaking resulting from a tilted core scenario is implied by the peaking factor or LHGR used in the analysis. There is no tilt multiplication factor applied to the peaking factors.

Assumptions

The Palisades FSAR specifically talks about three types of instabilities within the reactor core: radial, azimuthal and axial. This analysis is only concerned with the first two modes. It is assumed that the use of the word "radial" in the FSAR refers to an oscillation which moves from the center of the core outward to the periphery and then back. An oscillation of this type could be depicted by the top of a single spired circus tent being raised and lowered. It is assumed that the word "azimuthal" refers to an oscillation which traverses the entire width of the core before returning back to the point of origination. In the rigorous sense of the word, this type of oscillation could hypothetically traverse circumferentially around the core as well, much like a pie tin would rotate if it were not perfectly balanced on a central point.

The Palisades FSAR states that a radial oscillation in the reactor is highly unlikely and stable if it does occur. To this end, there are times when the word "radial" is used loosely, meaning either a truly radial oscillation, or sometimes meaning "about the radial plane". It is hoped that the context of the usage will clearly dictate the meaning.

There is one fundamental difference between the uncertainties derived from this analysis and the original values derived in the PIDAL Uncertainty Analysis which was brought on by the nature in which this analysis had to be performed. In the original PIDAL uncertainty analysis, it was assumed that the $S_{F(s)}$ uncertainty components contained both the measured and inferred components of the box power synthesis uncertainty. For this analysis, the $S_{F(s)}$ uncertainties calculated do not contain the same component because the detector powers supplied to PIDAL are based on theory. Since no data for significantly tilted cores exists for the Palisades reactor, it must be assumed that recalculating the uncertainty components based purely on theoretical detector powers is valid.

Analysis Methodology

In order to answer the questions posed by the NRC, it was necessary to supply PIDAL with incore detector signals from a variety of radially tilted configurations. It was desired to investigate the effects of quadrant power tilts on the order of 0% to 5%, as well as more severely tilted cases on the order of 10%.

The 0% to 5% tilt range was chosen because this covered the range over which the Palisades reactor can operate at greater than 25% power while remaining within the quadrant power tilt guidelines set forth in Palisades Technical Specification 3.23.3. At the present time, power operation with quadrant power tilts greater than 5% is not anticipated since tilts of this magnitude are highly unlikely unless a dropped control rod or otherwise severe localized power anomaly occurs. Nevertheless, it was deemed necessary to investigate how well PIDAL performed when more severe tilts were present.

Since Palisades rarely operates with measured quadrant power tilts greater than 1%, and measured incore detector signals for radially tilted cores were not available, it was necessary to find an alternate method for providing PIDAL with the required tilted incore detector data. It was decided to use detector powers derived from full core XTG solutions as input to PIDAL. This required that XTG cases be run which modelled radial or azimuthal imbalances in the reactor core.

A total of four XTG cases were run in order to model a variety of azimuthal and radial Xenon oscillation scenarios. Three of the four XTG runs started from a restart corresponding to roughly 3/4 total cycle length. The fourth case was run at BOC. These four cases all started the transient by dropping a single control rod into the core and then leaving the rod fully inserted for a period of 72 hours after which time the rod was rapidly pulled out. The ensuing transient was then followed for a period of 36 hours. The only differences between the four transient cases run were which control rod was dropped and therefore which direction the oscillation took across the core.

The first two of the transient cases were run by dropping group 3 control rods into the core. The first case dropped in a group 3-outer rod (rod 3-34) while the second case dropped in the central control rod (rod 3-33). The object of the case which dropped in the 3-outer rod was to induce an azimuthal oscillation. The object of dropping the central rod was to see if a radial oscillation could be induced.

The second two cases run both used a group 4 control rod as the transient initiator. The object of these two cases was to initiate an azimuthal oscillation which started off of the major axis (on a diagonal). Both of the two cases which used a dropped group 4 control rod as transient initiator were identical with the exception being that the first case was run at 3/4 cycle length while the second case was run at BOC.

Analysis Methodology

After the XTG cases were run, it was necessary to infer theoretical incore detector powers from the resultant three-dimensional XTG power distributions. This was accomplished by writing a small utility program, XTGDET, which used the power distribution from the XTG punch file as input.

The purpose of the XTGDET program was to read in a 3-D power distribution punch file created by XTG and convert the nodal powers into equivalent incore detector powers. Subroutine EXPAND is the meat of the XTGDET program. Based on the 3-D nodal power distribution determined by XTG, it calculates the theoretical detector powers. EXPAND uses the same methodology as subroutine EXPAND of PIDAL and Section 2.2.1 of the PIDAL Methodology Report should be consulted if further reference is required.

The XTGDET program was compiled and link edited four times. The program was identical for each compilation except for the incore detector location array, DETLOC. For the first compile DETLOC defined the actual locations of the detector strings in the reactor core (i.e. DETLOC was defined just like it was in the PIDAL block data section). For the second compilation the incore detectors spatial orientation to each other was not changed, but the entire core was rotated 90° clockwise underneath them. The third and fourth compiles rotated the core 180° and 270° clockwise respectively from its true orientation to the incore detector strings. The reason for wanting to rotate the core about the incore detector locations will be discussed shortly.

Once the theoretical detector powers were obtained for the radially tilted conditions, they were input to PIDAL. The core power distributions calculated by PIDAL were then compared back to the original XTG solution. For each of the PIDAL cases run, the statistical analysis option was chosen in order to determine the uncertainties associated with the PIDAL calculations for the tilted conditions.

Prior to discussing the actual PIDAL cases which were run, it is appropriate to describe the temporary modifications which were made to the cycle 7 PIDAL model in order to overlay the measured incore detector signals with the full core theoretical values supplied by XTG via XTGDET. In the main program, immediately after the call to Subroutine BXPWR (which calculates the detector powers based on measured millivolt signals and the Wprimes), temporary coding was added which reads in the theoretical detector powers and detector level normalization factors produced by XTGDET. This read was activated by the IXPOW flag which is normally used to tell PIDAL to use theoretical detector powers from the 1/4 core XTG model that runs concurrently with each PIDAL case. Following the input of the full core theoretical detector powers, the IXPOW flag was turned off so that the normal 1/4 core theoretical detector power logic in PIDAL would not take effect. Note that the measured detector powers are actually overlaid by the new coding and that PIDAL assumes the full core theoretical values to be measured from this point on.

Analysis Methodology

A total of 19 PIDAL cases were run for this analysis. The first case was a non-tilted base case which corresponds to the core conditions at 3/4 EOC. The XTG case used to supply the full core theoretical detector powers was the second step of the 3/4 EOC group 4 rod drop scenario. The base case is important because it serves to verify that the entire system is working as designed for this analysis. The following checks were made:

- Verification that the full core XTG model for cycle 7 is working properly by comparing the full core XTG run with the 1/4 core XTG power distribution of PIDAL.
- Verification that the XTGDET program is working properly by comparing the full core XTG power distribution with the XTGDET collapsed 2-D radial power distribution.
- Verification that the XTGDET program is working properly by comparing the XTGDET theoretical detector powers with those previously calculated by the 1/4 XTG which is part of PIDAL.
- Verification that the full core detector signals are getting input to PIDAL correctly from XTGDET and that the PIDAL solution is correct by comparing the PIDAL solution with the original XTG solution.

With description of the base case out of the way, discussion on the remaining 18 PIDAL cases is appropriate. The PIDAL cases run used theoretical detector powers from two of the XTG dropped rod induced transient scenarios. The first 6 PIDAL cases used powers from the 3/4 EOC group 4 rod induced transient while the second 6 used powers from the group 3-outer rod induced XTG case.

The first six PIDAL cases run corresponded to peak quadrant power tilts of 10%, 7.6%, 5.6%, 2.9%, 1.6% and 0.3% respectively. These cases were selected because they covered the spectrum of tilted cores for a tilt range of no tilt up to 10% tilt. Concentration on tilts between 0% and ~5% was greater because it is over this range that the reactor may be operated without reducing power or correcting the tilt. The second six PIDAL cases all lie within the no tilt and ~5% quadrant power tilt range.

Analysis Methodology

There were two reasons for using the two different transient scenarios as suppliers of the theoretical detector powers. First, the dropped group 3-outer rod scenario did not result in quadrant power tilts greater than 5% during the oscillatory period. Therefore, it was necessary to use cases from the dropped group 4 rod scenario in order to get results on tilts up to 10%. Secondly, the oscillations between the two scenarios were quite different. The dropped group 3-outer rod oscillated about the major symmetric axis while the dropped group 4 rod scenario oscillated about the diagonal axis. Consideration of both is important because the majority of the symmetric incore detector locations are rotationally symmetric (and not generally symmetric about either major axis or diagonal) and therefore oscillations about differing axis' could have differing effects on the accuracy of the PIDAL quadrant power tilt algorithm.

Expanding on this last statement, it was decided to further investigate the effects of tilt location on the PIDAL solution. In the case of the dropped group 4 rod induced transient, the power peak used for the PIDAL cases 1 through 6 occurred in quadrant 2. What if the power peak was in one of the other three quadrants? In other words, what if the power distribution was the same, just rotated 90°, 180° or 270°? Since the incore detectors are not equally distributed over the quadrants, it is not expected that the power distributions as measured by PIDAL would be the same for the rotated cases. The same questions can be asked for the group 3-outer rod induced transient as well.

The XTGDET program allowed for use of the same XTG case for each of the four possible symmetric oscillations induced by individually dropped group 4 rods. In a similar fashion, the existing group-3 outer dropped rod XTG case could be used for three additional symmetric transient scenarios.

Six additional PIDAL cases were then run. Three of the cases were for the 5% tilted group 4 rod induced oscillation at rotations of 90°, 180° and 270° clockwise from the original power distribution. The other three cases were for the 5% tilted group 3-outer rod induced transient at rotations of 90°, 180° and 270°.

Analysis Results

The results of the three transient cases which caused azimuthal xenon transients are summarized in Table #1. From this table it is apparent that the core is less stable at beginning of cycle than at EOC azimuthally. This is in agreement of Section 3.3.2.8 of the Palisades FSAR which states that it appears that the azimuthal mode is the most easily excited at beginning of life even though the axial mode becomes the most unstable later. From Table #1 it is also clear that the oscillation resulting from the group 4 rod drop is more severe from a quadrant power tilt standpoint than for the group 3-outer rod drop. The reason for this is that in the group 3-outer induced transient, the power peaking is symmetric along the quadrant lines, and therefore the peak tilt is actually distributed over two adjacent quadrants. In the case of the dropped group 4 rod transient, the power peaking is symmetric about the diagonal which lies within a single quadrant.

Table #2 presents the results of the PIDAL cases which were run and it is this data that will be used to answer the questions asked by the NRC. The first NRC request was for comparison of the tilt measured by PIDAL with the true or theoretical tilt. For the dropped group 4 rod case, the agreement between the PIDAL solution and the original XTG quadrant power tilt was very good: For the true tilts between 0% and 10%, the error was on the order of 0.72% or less.

For the dropped group 3-outer rod induced transient, the quadrant power tilt was not as accurately measured, however it was measured conservatively in each case. For true quadrant power tilts of ~4% or less, the PIDAL tilt was still within 1% of the original XTG. When the true tilt rose to greater than 5% the error in the PIDAL tilt calculation reached 1.23%. Again it should be noted that the PIDAL tilt for these cases was always higher than the true tilt and therefore conservative.

The second NRC comment asked that the PIDAL code programming be verified correct by supplying theoretical detector input and comparing the resulting PIDAL solution with the original theoretical power distribution solution. In actuality, this comment had already been addressed by the PIDAL Uncertainty Analysis. The $S_{F(r)}$ uncertainty component represents the error in the PIDAL solution when PIDAL is given detector powers from a known power distribution solution. For the entire data base, the $S_{F(r)}$ uncertainty component was 0.0022. This value is in excellent agreement with the individual case $S_{F(r)}$ uncertainty components found on the statistical summary edit following each of the PIDAL runs performed for this analysis.

Analysis Results

The third comment made by the NRC requested that a determination of the $S_{F(s)}$ uncertainty component for tilted cores be made. To this end, the PIDAL statistical analysis routines, which calculate the individual case uncertainty components, were activated for each of the eighteen tilted core PIDAL runs made. The individual results are presented in Table #2. When looking at these values, the reader should keep in mind the overall $S_{F(s)}$ uncertainty component of 0.0277 for the entire data base arrived at in PIDAL Uncertainty Analysis. Based on the results presented in Table #2 it can be concluded that the uncertainty component $S_{F(s)}$ bounds core measurements up to quadrant power tilts of 2.8% (linear interpolation between cases 9 and 10). Furthermore, depending on the direction of the oscillation, the PIDAL measurements are bounded to above the current 5% quadrant power tilt Technical Specification limit.

For the oscillation symmetric about the core diagonal, the PIDAL measurement uncertainty previously determined is valid for tilts up to 5%. For the oscillation about the core major axis, the $S_{F(s)}$ uncertainty component ceases to bound the value assumed in the PIDAL uncertainty analysis for quadrant power tilts greater than 2.8%. This means that the uncertainties derived in the PIDAL Uncertainty Analysis are not valid for all cases when quarter core tilts are greater than 2.8%.

Because it was shown that the current uncertainties do not bound all tilted cases, it was necessary to find new uncertainties which take power distributions with tilts greater than 2.8% into account. This was done by utilizing the PIDAL statistical processor program, to combine the data from PIDAL cases 13 through 18. The PIDAL statistical program, which was developed and documented as recorded in the PIDAL Uncertainty Analysis, can take statistical data output by individual PIDAL cases and combine it to represent an entire population. Cases 13 through 18 were used as the basis for the new tilted core uncertainty because they all were based on theoretical tilts of roughly 5% (actually 5.58% and 5.11%). The 5% quadrant power tilt cut-off was specified because Technical Specification 3.23.3 allows for full power operation of the reactor for quadrant power tilts up to 5%, without any compensatory action.

The results of the statistical combination for the tilted cases may be found in Table #3. The non-tilted data presented is taken from the previous PIDAL Uncertainty Analysis. The F_r^q , $F_r^{A_h}$ and F_r^A data presented in Table #3 is the basis for the revised Technical Specification Table 3.23.3.

In response to the fourth NRC comment, a discussion on how quadrant power tilt effected the Palisades Safety Analysis took place with members of the Palisades Transient Analysis Group. It was learned that quadrant power tilt is not an input to the Safety Analysis and that the increase in local or radial peaking resulting from a tilted core scenario is implied by the peaking factor or LHGR used in the analysis. There is no tilt multiplication factor applied to the peaking factors.

Analysis Results

Table #1

Step	Hours from drop	Group 3-Outer 3/4 EOC TILT	Group 4 3/4 EOC TILT	Group 4 BOC TILT
1	0	1.0000	1.0000	1.0000
2	0	1.0627	1.0708	1.0708
3	72	1.0488	1.0542	1.0505
4	73	1.0191	1.0410	1.0458
5	74	1.0329	1.0697	1.0777
6	75	1.0424	1.0892	1.1011
7	76	1.0483	1.1007	1.1162
8	77	1.0510	1.1057	1.1238
9	78	1.0511	1.1054	1.1251
10	79	1.0495	1.1013	1.1212
11	80	1.0459	1.0941	1.1133
12	81	1.0416	1.0854	1.1025
13	82	1.0369	1.0757	1.0898
14	83	1.0318	1.0657	1.0761
15	84	1.0266	1.0558	1.0621
16	85	1.0217	1.0463	1.0484
17	86	1.0171	1.0374	1.0354
18	87	1.0129	1.0294	1.0236
19	88	1.0092	1.0222	1.0132
20	89	1.0060	1.0160	1.0043
21	90	1.0033	1.0108	1.0104
22	91	1.0011	1.0065	1.0145
23	92	1.0006	1.0030	1.0173
24	93	1.0018	1.0036	1.0189
25	94	1.0027	1.0045	1.0194
26	95	1.0033	1.0051	1.0190
27	96	1.0036	1.0054	1.0177
28	97	1.0038	1.0054	1.0159
29	98	1.0037	1.0053	1.0136

Table #1 - Peak quadrant power tilts for three scenarios each initiated by dropping a control rod, leaving it inserted for 72 hours and then rapidly withdrawing it. Values predicted by Palisades cycle 7 full core XTG model.

Analysis Results

Table #2

Case	Initiating Rod	XTG Tilt	PIDAL Tilt	% Tilt Error	S _{F(s)}	S _{F(sa)}
BASE	-----	1.0000	1.0000	0.0000	0.0010	0.0008
1	4	1.1013	1.0959	-0.54	0.0376	0.0321
2	4	1.0757	1.0721	-0.36	0.0280	0.0242
3	4	1.0558	1.0533	-0.25	0.0198	0.0180
4	4	1.0294	1.0284	-0.10	0.0101	0.0102
5	4	1.0160	1.0158	-0.02	0.0077	0.0066
6	4	1.0030	1.0037	0.07	0.0089	0.0044
7	3-Outer	1.0511	1.0634	1.23	0.0495	0.0445
8	3-Outer	1.0416	1.0520	1.04	0.0409	0.0367
9	3-Outer	1.0318	1.0403	0.85	0.0313	0.0289
10	3-Outer	1.0217	1.0282	0.65	0.0219	0.0211
11	3-Outer	1.0092	1.0132	0.40	0.0112	0.0112
12	3-Outer	1.0006	1.0014	0.08	0.0083	0.0035
13	4	1.0558	1.0486	-0.72	0.0239	0.0217
14	3-Outer	1.0511	1.0606	0.95	0.0529	0.0476
15	4	1.0558	1.0533	-0.25	0.0207	0.0188
16	3-Outer	1.0511	1.0634	1.23	0.0490	0.0439
17	4	1.0558	1.0486	-0.72	0.0228	0.0205
18	3-Outer	1.0511	1.0606	0.95	0.0533	0.0480

Table #2 - Quadrant power tilts and detector power uncertainty components for for PIDAL for radially tilted cores.

Note: For all scenarios, PIDAL correctly identified the quadrant in which the maximum quadrant tilt occurred.

Cases 13 and 14 were for a core rotated 90° CW under the incores.

Cases 15 and 16 were for a core rotated 180° CW under the incores.

Cases 17 and 18 were for a core rotated 270° CW under the incores.

Analysis Results

Table #3

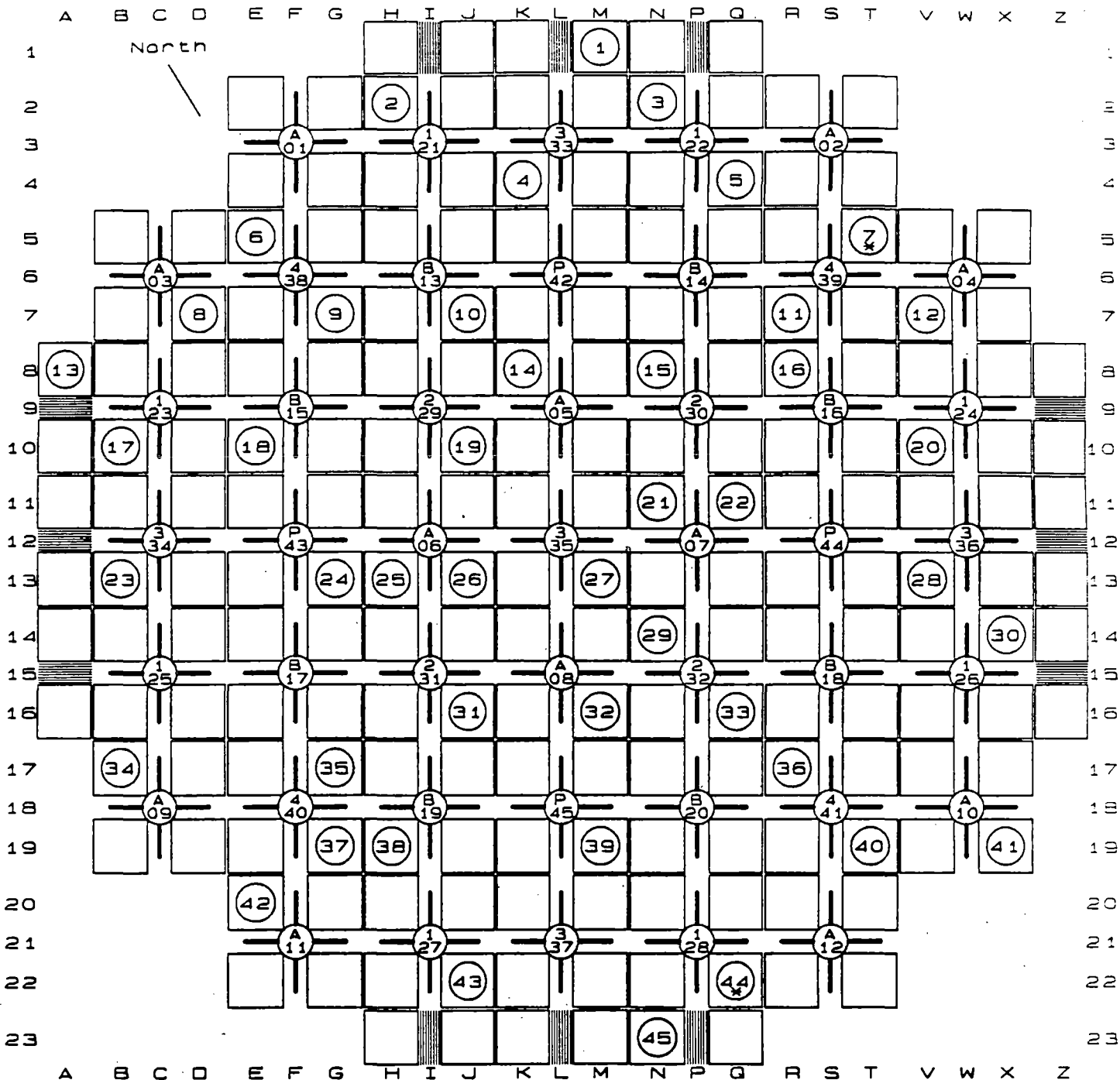
Statistical Variable	Standard Deviation	Degrees of Freedom	Tolerance Factor	Tolerance Limit
F(s) #	0.0393	1800	---	---
F(sa) #	0.0351	360	---	---
F(r) #	0.0026	408	---	---
F(s) *	0.0306	3415	---	---
F(sa) *	0.0241	683	---	---
F(r) *	0.0021	969	---	---
F(s)	0.0277	8768	---	---
F(sa)	0.0194	1754	---	---
F(r)	0.0022	2754	---	---
F(z)	0.0151	1122	---	---
F(L)	0.0135	188	---	---
F ^q #	0.0443	2487	1.703	0.0795
F ^{Δh} #	0.0383	489	1.766	0.0722
F _r ^A #	0.0352	364	1.785	0.0695
F ^q *	0.0368	3822	1.692	0.0664
F ^{Δh} *	0.0277	877	1.733	0.0526
F _r ^A *	0.0242	694	1.746	0.0490
F ^q	0.0344	4826	1.692	0.0623
F ^{Δh}	0.0237	1225	1.727	0.0455
F _r ^A	0.0195	1790	1.712	0.0401

Table #3 - Summary of PIDAL Statistical Component Uncertainties.

- # -- values to be used when quadrant power tilt exceeds 2.8% but is less than or equal to 5%.
- * -- values for cores with once-burnt reused incore detectors.

Note: For the final tolerance limits, penalty factors of .0041, .0046 and .0067 for F^q, F^{Δh} and F_r^A respectively were included to account for up to 25% incore detector failures.

Palisades Nuclear Plant Reactor Core Plan



Form from EGAD 13 revision 0